Renewable and Sustainable Energy Reviews 167 (2022) 112798

Contents lists available at ScienceDirect

Renewable and Sustainable Energy Reviews

journal homepage: www.elsevier.com/locate/rser

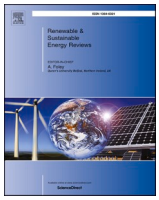

High-temperature and transcritical heat pump cycles and advancements: A review

Keri-Marie Adamson [a], Timothy Gordon Walmsley [a,*], James K. Carson [a], Qun Chen [b], Florian Schlosser [c], Lana Kong [a], Donald John Cleland [b]

[a] Ahuora – Centre for Smart Energy Systems, School of Engineering, University of Waikato, Hamilton, 3240, New Zealand
[b] Massey University, Private Bag 11-222, Palmerston North, 4420, New Zealand
[c] Department of Energy Systems Technologies, University of Paderborn, Paderborn, Germany

ARTICLE INFO

Keywords:
High-temperature heat pump
Transcritical heat pump
Vapour compression cycle
Process integration

ABSTRACT

Industrial and large-scale heat pumps are a well-established, clean and low-emission technology for processing temperatures below 100 °C, especially when powered by renewable energy. The next frontier in heat pumping is to extend the economic operating envelope to supply the 100–200 °C range, where an estimated 27% of industrial process heat demand is required. Most high-temperature heat pump cycles operate at pressures below the refrigerant's critical point. However, high-temperature transcritical heat pump (HTTHP) technology has - due to the temperature glide – a significant efficiency potential, especially for processes with large temperature changes on the sink side. This review examines how further developments in HTTHP technology can leverage innovations from high-temperature heat pump research to respond to key technical challenges. To this end, a comprehensive list of 49 different high temperature or transcritical heat pump cycle structures was compiled, which lead to classification of 10 performance-enhancing cycle components. Focusing specifically on high-temperature transcritical heat pump cycles, this review establishes six technical challenges facing their development and proposes solutions for each challenge, including a new transcritical-transcritical cascade cycle innovation. A key outcome of the review is the proposal of a new cycle that requires detailed investigation as a candidate for a high-temperature transcritical heat pump cycle.

1. Introduction

Energy consumption and generation is a significant part of the global economy. In 2019, the supply of global primary energy reached 162,000 TWh, of which 84.5% (137,000 TWh) was supplied using fossil fuels [1]. With the need to decarbonise becoming ever more pressing, it is important to understand the global energy demand profile to develop effective low-emissions solutions for large energy consumers. An estimation of the total global energy demand for 2019 is presented in Fig. 1 [2].

While industrial process heat only contributes 19% of the total energy demand, it accounts for 36.8% (12.3 Gt CO_2-e) of the total energy-related emissions due to the large proportion of energy supplied by fossil fuel boilers [4]. Global milestones, established by The International Energy Agency (IEA), to achieve net-zero greenhouse gas emissions by 2050 will require industries to switch from fossil fuels to more sustainable and renewable sources [5]. One of these milestones outlines the transition to a 40% larger world economy while consuming 7% less energy by 2030, which would require wind and solar electricity generation to increase by a factor of four and the uptake of 'clean' technologies to increase by a factor of 18 to decrease the energy intensity of GDP by 4% per year.

At the forefront of 'clean' technologies in the industrial energy transition is heat pump (HP) technology [6]. By utilising electricity, HPs can make use of 'waste heat' that is available in many processing industries [7] to reduce the overall energy demand from fossil fuel boilers and therefore reduce emissions, particularly when powered by renewable electricity. Zhu et al. [8] included HPs as one of six essential smart energy systems technologies. Further, Worrell and Boyd [9] applied a bottom-up approach to identify deep decarbonisation pathways for U.S. manufacturing where HPs enabled 22% of emission reductions based on a near-zero electricity grid.

HP technology is a well-established for commercial and residential applications [10], district heating [11], and industrial process heat [12] for temperatures below 100 °C. HPs can provide flexibility for energy

* Corresponding author.
E-mail address: tim.walmsley@waikato.ac.nz (T.G. Walmsley).

https://doi.org/10.1016/j.rser.2022.112798
Received 17 April 2022; Received in revised form 22 June 2022; Accepted 18 July 2022
Available online 12 August 2022

Nomenclature

h	Enthalpy, kJ/kg
P	Pressure, MPa
s	Entropy, kJ/kg-K
T	Temperature, K

Abbreviations

CFC	Chlorofluorocarbons
COP	Coefficient of Performance
GDP	Gross Domestic Product
GWP	Global warming potential
HCFC	Hydrochlorofluorocarbons
HCFO	Hydrochlorofluoroolefin
HFC	Hydrofluorocarbons
HFO	Hydrofluoroolefin
HP	Heat pump
HTHP	High-temperature heat pump
HTTHP	High-temperature transcritical heat pump
IHX	Internal heat exchanger
ODP	Ozone depleting potential

grid systems as a demand-side response and management tool [13], which would enable greater uptake of intermittent renewable energy technologies, e.g., wind turbine and HP hybrid systems [14] and flexible utility systems [15]. The addition of thermal storage and system optimisation can enable high efficiency operation, thereby minimising required capital investment in industrial-scale HPs [16].

High-temperature heat pump (HTHP) technology is much less established with limited commercially available units. For the 100–200 °C process heating range where 27% of industrial process heat demand exists (Fig. 1), Arpagaus et al. [17] identified many promising HP applications, including drying, thermal separation and preservation in the food, paper, chemical, metal and plastic manufacturing sectors, that rely on steam heating from fossil fuel boilers. Most HP research in the open literature only covers heat sink temperatures up to 160 °C with relatively few studies going beyond this temperature. In this review, HTHPs are defined as those with heat sink temperatures above 100 °C [17], which has sometimes been referred to as very high-temperature or ultra-high-temperature heat pumps in other studies, e.g., Ref. [18]. Within HTHPs, there are sub-critical cycles, which require refrigerants with a high critical temperature (e.g., >120 °C), and transcritical cycles, which intentionally compress the refrigerant beyond its critical point and release heat in a gas cooler.

Recent HP reviews have focussed on industrial-scale HTHPs, transcritical heat pumps and natural refrigerants (Table 1). Refrigerant development and evaluation have been a major focus of much HTHP research and reviews due to its direct effect on cycle performance and the need for phase-out of high global warming potential (GWP) and ozone depleting potential (ODP) refrigerants [19]. In contrast, a systematic review and compilation of all the potential HTHP cycle structures is needed with a focus on identifying and developing cycles that would be appropriate for HTTHP technology.

This current review aims to identify research gaps and opportunities in the emerging field of HTTHP technologies (heat sink >100 °C) and their integration. To achieve this aim, the fundamental concepts of HP cycles are presented to identify how each of the essential processes (expansion, heat exchange and compression) may be enhanced to achieve greater performance and higher temperatures. Subsequently, the review focuses on how these enhancement opportunities have been exploited in practice and finally the challenges and potential solutions to the advancement of HTTHP cycles (which have not been comprehensively reviewed to-date) are covered.

The paper contributes to the literature in the following ways:

- Presents a comprehensive collation (with performance metrics) of 49 different sub-critical and transcritical HP cycles.
- Identifies the potential of transcritical HP cycles for high-temperature (heat sink >100 °C) applications including an original new cycle structure.
- Proposes key research directions including the need to combine process integration and HP cycle development to maximise energy efficiency (COP) and minimise greenhouse gas emissions.

2. Heat pump fundamentals and components

The components and operation of a basic HP cycle are different from other types of heating systems such as furnaces, boilers and electrical heating systems that generate heat. HPs absorb heat into a refrigerant (also commonly referred to as the working fluid) at a low temperature

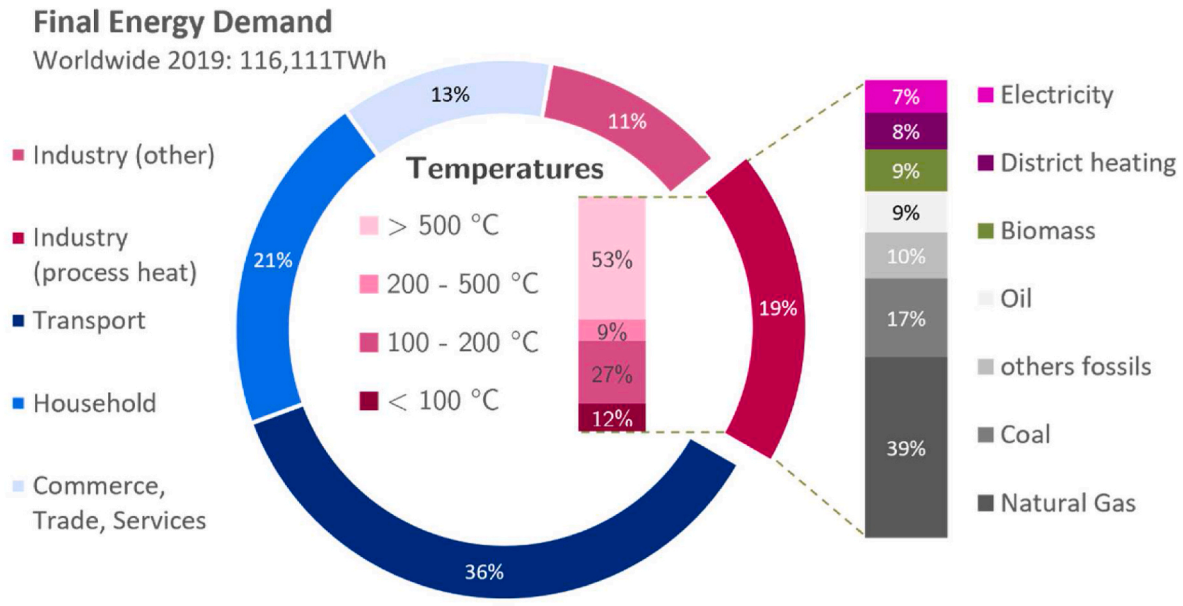

Fig. 1. Global final energy demand in 2019 by sector [2] with estimates for application temperatures and final energy sources [3].

Table 1
Existing heat pump review papers (between 2010 and 2021).

Review paper	Industrial-scale applications	High-temperature heat pumps (above 100 °C)	Transcritical heat pumps	Natural Refrigerants, HFO, Hydrocarbons	High-temperature transcritical heat pumps (above 100 °C)
Jesper et al. [7]	✓✓	✓	–	✓	–
Zhang et al. [12]	✓	–	–	✓	–
Sarkar [20]	–	–	✓	–	–
Arpagaus et al. [17]	✓	✓✓	–	✓	–
Wu et al. [21]	✓	✓	–	✓✓	–
Chua et al. [22]	✓	–	–	✓	–
Schlosser et al. [23]	✓	–	–	–	–
Arpagaus et al. [24]	–	–	✓	✓	–
Bamigbetan et al. [25]	✓	✓	–	✓✓	–
Gaur et al. [26]	–	–	–	✓	–
Goyal et al. [27]	✓	–	–	–	–
Ma et al. [28]	✓	–	✓	✓	–
Fischer and Madani [29]	–	–	–	–	–
Sarbu [30]	✓	–	–	✓	–
Cao et al. [31]	–	–	✓	–	–
Lecompte et al. [32]	✓	–	✓	✓	–
Huang et al. [33]	✓	–	–	–	–
Menon et al. [34]	✓	–	–	–	–
Mohanraj et al. [35]	–	–	–	✓✓	–
Austin and Sumathy [36]	✓	–	✓✓	✓	–
Schlosser et al. [37]	✓✓	✓	✓	✓	–
Jiang et al. [38]	✓	✓✓		✓	

✓✓ Comprehensively reviewed, Main review focus
✓ Comprehensively reviewed
– Not mentioned or mentioned but not reviewed

(the 'source') followed by compression of the fluid that is accompanied by an increase in temperature, and subsequent rejection of the heat at the higher temperature (the 'sink'). To close the cycle, an expansion process returns the fluid to its original state (i.e., original temperature, pressure, enthalpy, entropy) before re-entering the heat absorption process. In this way, the 'waste' heat from a stream in an industrial process, or heat from the environment, can be upgraded and utilised in other processes at the cost of work input.

The COP expresses the thermodynamic performance of a HP system and is defined as the quantity of heat transferred to the heat sink divided by the quantity of work input to the compressor (Eq. (1)). The COP of a HP normally exceeds 1 and can be as high as 5 or 6 for indirect closed cycles and >10 for direct compression in an open cycle [39]. By contrast, industrial boilers achieve typical thermal efficiencies of 80%–90%, effectively equivalent to a COP of up to 0.90.

$$COP_{HP} = \frac{Q_H}{W} \tag{1}$$

Minimising compression work (W) while still achieving the heat sink target temperature and heat flow rate (Q_H) will result in increased COP values.

The following sections explain the theory of the HP cycle and discuss the key components of expansion, compression, heat exchange, and refrigerant. This provides a context for the classification and discussion of HP cycles and performance advancement options.

2.1. Fundamentals of the heat pump cycle

A HP cycle that makes use solely of thermodynamically reversible processes (with the most common example being the reverse Carnot cycle [40]) can achieve the highest COPs for given source and sink temperatures [41]. The reverse Carnot cycle is an ideal cycle that comprises the following stages (Fig. 2): 1–2 an isentropic process during which a refrigerant is compressed adiabatically, 2–3 an isothermal compression process (during which heat is rejected to a sink at T_H), 3–4 an isentropic expansion process during which a refrigerant is expanded adiabatically, 4–1 an isothermal expansion process (during which heat is absorbed from a heat source at T_C) that returns the refrigerant to its

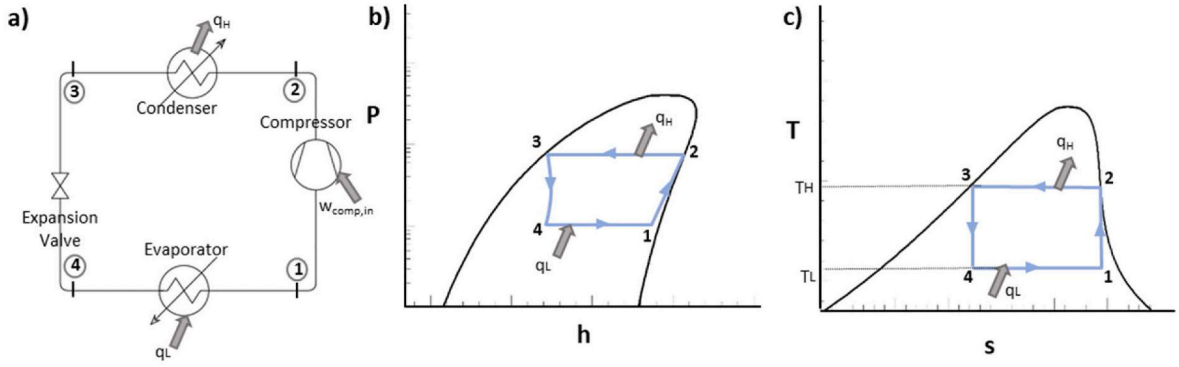

Fig. 2. (a) Carnot cycle schematic illustrated using (b) P-h and (c) T-s diagrams.

original state. Fig. 2 shows the four stages of a Carnot cycle plotted on temperature-entropy (T-s) and pressure-enthalpy (P-h) phase diagrams, where the black curve represents the saturation region (i.e., liquid and vapour saturation lines) and the blue lines represent the cycle stages.

The COP of a Carnot HP cycle may be related directly to the source and sink temperatures:

$$COP_{HP} = \frac{Q_H}{W} = \frac{T_H \Delta s}{(T_H - T_L)\Delta s} = \frac{T_H}{T_H - T_L} \quad (2)$$

where T_H is the absolute temperature of the heat sink, T_L is the absolute temperature of the heat source and Δs is the entropy change of the refrigerant during the isothermal heat absorption and rejection processes. Eq. (2) shows that the COP of a Carnot HP increases with increasing heat sink temperature (T_H) and decreases as the temperature lift (i.e., the temperature difference between the heat sink and source temperatures, $T_H - T_L$), increases, and this is also generally true of practical HP cycles. As the processes in a reverse Carnot cycle are reversible, its performance is independent of the thermodynamic properties associated with different refrigerants [42].

The Carnot HP (or refrigeration) cycle, which involves reversible compression of a two-phase fluid mixture, is physically impossible to achieve in practical systems. As a result, most real HPs operate on the vapour compression cycle (reverse-Rankine cycle) with isenthalpic rather than isentropic expansion as shown in Fig. 3 [41].

As the heat transfer, compression and expansion processes in real vapour-compression cycles are irreversible, the COP of a vapour compression cycle cannot be as high as that of a Carnot cycle operating between the same source and sink temperatures. In practice, real HP cycles have achieved up to 60% of the Carnot cycle COP [41].

The majority of HPs operate a subcritical vapour compression cycle where the heat is rejected below the refrigerant's critical temperature and pressure as it condenses, as illustrated in the pressure-enthalpy (P-h) diagram in Fig. 4a [36]. By contrast, a transcritical cycle rejects heat at pressures above the critical pressure of the refrigerant through sensible cooling of a single supercritical phase in a gas cooler (Fig. 4b) rather than a condenser. The advantages of rejecting heat in the supercritical region are that the outlet temperature and pressure of the gas cooler are not interdependent (i.e. there are two degrees of freedom compared to one in the two-phase envelope) [36], which gives a greater scope for optimisation. The temperature glide of the refrigerant through the gas cooler is significantly greater than that across a condenser (subcritical cycle). Closer matching of the refrigerant temperature glide to the heat sink load temperature profile can reduce entropy generation and, more importantly, power consumption compared to a subcritical cycle equivalent [43]. As for subcritical cycles, the heat absorption in a transcritical cycle occurs via phase change of the refrigerant in an evaporator.

As transcritical cycles involve significant temperature glide in the gas cooler, the Lorenz cycle [44], rather than the Carnot cycle, is the more appropriate ideal cycle to compare performance against. While the Carnot cycle operates between constant temperatures T_{H1} and T_L, the Lorenz cycle may be thought of as a series of Carnot cycles where each cycle has an infinitesimally lower sink temperature than the neighbouring cycle for the temperature glide from T_{H1} to T_{H2}. As a result, the Lorenz COP can be calculated by replacing T_H in Eq. (2) with the logarithmic mean ($T_{H,m}$) of T_{H1} and T_{H2}, Eq. (3). If there is a glide on source side in the HP cycle, the logarithmic mean of the lower temperatures would also apply (e.g., reverse Brayton cycle).

$$T_{H,m} = \frac{T_{H1} - T_{H2}}{\ln\left(\frac{T_{H1}}{T_{H2}}\right)} \quad (3)$$

The pressure-enthalpy-temperature relationships of refrigerants depend on the molecular structure and composition of the refrigerant. Fig. 5, for example, demonstrates the stark contrast between the pressure-enthalpy relationship for isobutane and ammonia. The clearest difference between the two is the shape of the two-phase envelope under the saturation (curved black) line, with isobutane having the 'skewed' appearance characteristic of hydrocarbons, while ammonia has a more 'rounded' shape like other low-molecular-weight fluids, such as water and carbon dioxide. The slope of the liquid saturation line (i.e., the portion of the saturation curve to the left of the critical point) has a significant effect on throttling losses, with losses increasing as the slope of the liquid saturation line decreases [42]. For vapour saturation curves like that of isobutane, significant superheating of the vapour before compression is required to prevent liquid droplets from forming in the compressor, which is often referred to as "wet compression" (Section 3.3). A second observation is the contrasting isotherm shapes in the region above the critical point. For transcritical cycles (examples shown in red), the shape of the isotherms in the region above the critical point affects how well the refrigerant temperature profile matches the heat sink temperature profile.

Thermodynamic inefficiencies, or entropy generation, can occur in each stage of a standard vapour compression cycle. They can be reduced by adding cycle components and selecting a suitable refrigerant for the given source and sink temperatures. Each stage of the cycle is considered separately in the following subsections.

2.2. Expansion

In the standard vapour compression cycle, the refrigerant is expanded freely and irreversibly (throttled) without recovering work from the expansion process (unlike the Carnot cycle). Throttling losses occur due to friction in the valve which expends the expansion energy [45]. Throttling losses are variable depending on the properties of the refrigerant, with higher heat capacity refrigerants tending to incur larger throttling losses [42]. In a subcritical vapour compression cycle,

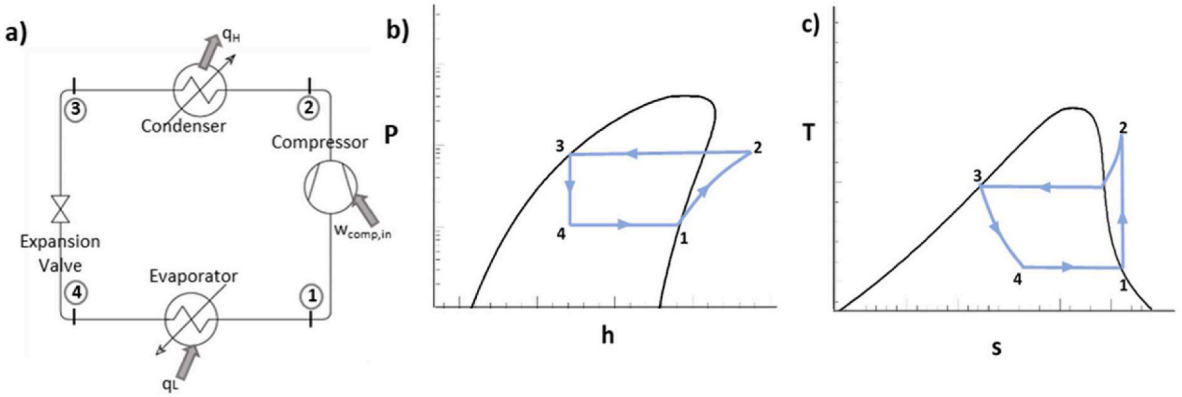

Fig. 3. (a) Reverse Rankine vapour compression cycle schematic illustrated using (b) P-h and (c) T-s diagrams.

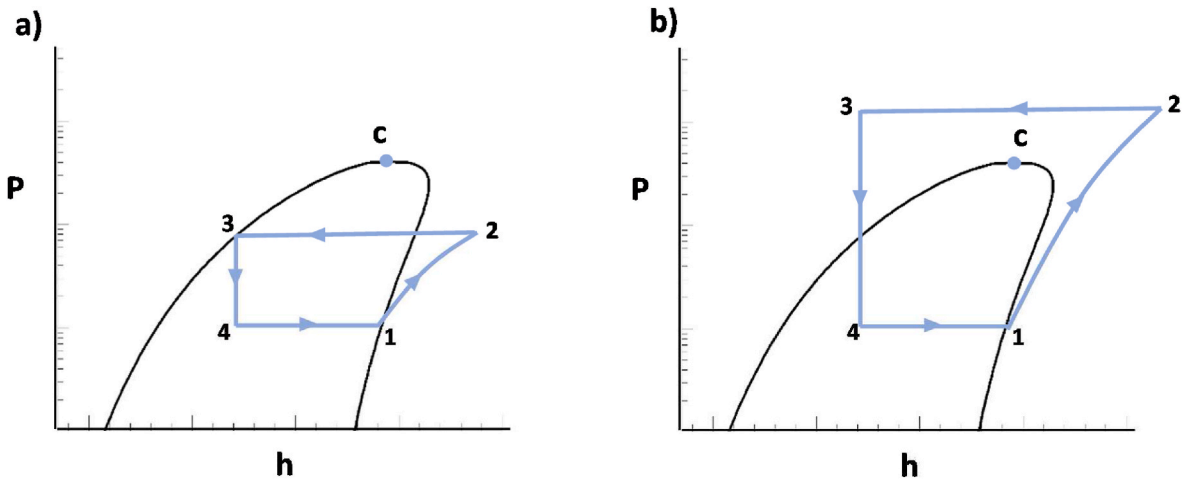

Fig. 4. Pressure-enthalpy diagrams displaying (a) subcritical heat pump cycle, (b) Transcritical heat pump cycle. Showing compression (1–2), condenser (2–3), gas cooler (2–3), expansion valve (3–4), evaporator (4–1), and critical point (C).

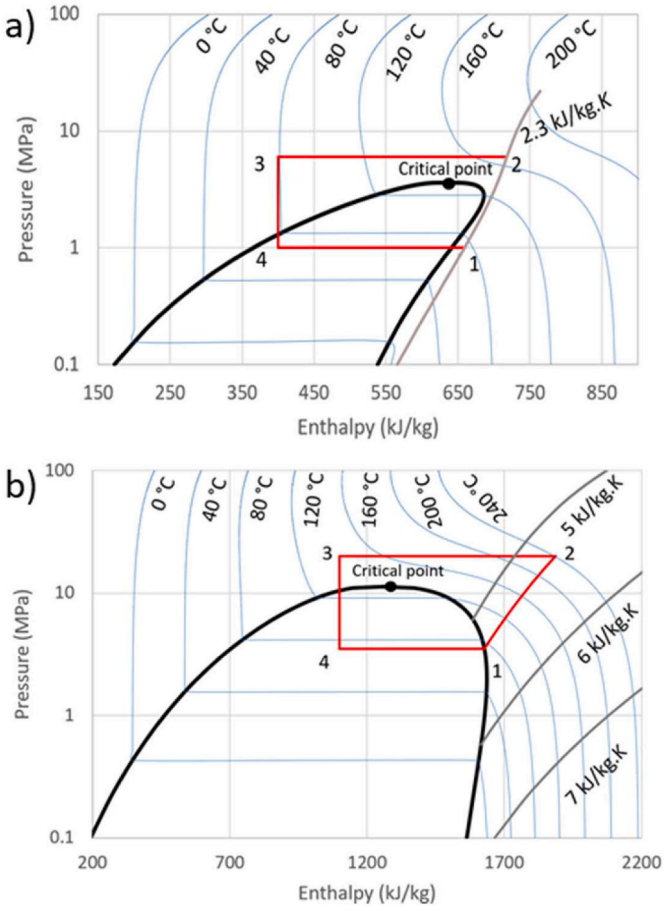

Fig. 5. (a) Isobutane (R600a) P-h diagram with isotherms and (b) Ammonia (R717) P-h diagram with isotherms and isentropes.

the refrigerant should be fully condensed as a saturated or sub-cooled liquid as it enters the expansion device to ensure effective and consistent operation since they are designed to receive a high-density single phase. The amount of gas formed during the expansion ('flash gas') reduces both refrigeration and heating capacity for the same total flow rate of refrigerant and compressor work, as well as the COP.

Throttling losses can be reduced by:

(1) Subcooling the refrigerant

The amount of flash gas in subcritical systems may be reduced by subcooling the refrigerant before expansion [46]. Subcooling is often achieved through internal heat exchange (IHX) that superheats the compressor suction gas. With increasing degrees of subcooling, there is a maximum COP (depending on the refrigerant) that can be achieved due to the trade-off between increased compression work as compressor suction superheat increases and increased evaporator enthalpy difference due to reduced flash gas requiring a lower refrigerant mass flow for the cooling duty [46].

For some transcritical cycles, depending on the refrigerant, the quality of the refrigerant (i.e. the fraction of refrigerant that is in the vapour state) exiting the expansion valve can be higher than for subcritical systems resulting in comparatively greater throttling losses [45]. These losses increase with increasing gas cooler outlet temperature [47]. Consequently, multistage expansion and expansion work recovery (discussed below) can have a comparatively greater effect on improving transcritical cycle COPs than for subcritical cycles.

(2) Multistage expansion

When significant flash gas is present, efficiency can be improved by using multi-stage expansion (Section 3.3). With multi-stage expansion, the flash gas from the high stage expansion is compressed from an intermediate suction pressure, thereby reducing compression work relative to a single-stage expansion where all the flash gas must be compressed across the full pressure lift.

(3) Expansion work recovery (expanders or ejectors)

Expansion work can be partially recovered by the addition of ejectors or expanders. Several expander devices have been developed, including scroll-type expanders [48], reciprocating expanders [49], double rolling piston expanders [50], turbo expanders [51], and vane-type expanders [47]. However, according to Zhang et al. [45], commercial uptake of expander technology has been slow. For most cycles, the expansion results in the refrigerant entering the two-phase region which can negatively affect the mechanical integrity of the expander compared to single-phase expansion (standard technology).

Ejectors are used in conjunction with flash vessels (refer to Arpagaus et al. [24] for multiple cycle arrangements) and are analogous to injector systems in steam engines in that they mix high- and low-pressure fluids to output an intermediate pressure fluid. An ejector chamber includes three stages, the nozzle stage, the mixing stage and the diffusing stage

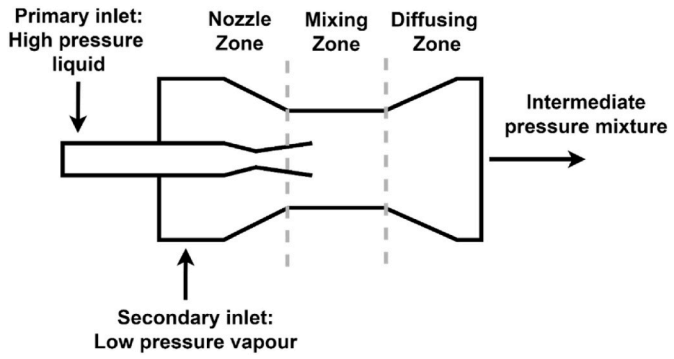

Fig. 6. Simple ejector schematic [20].

(Fig. 6). The high-pressure refrigerant enters the nozzle, converting hydraulic pressure into kinetic energy that accelerates the refrigerant, and the high-velocity vapour at the nozzle exit entrains the low-pressure refrigerant entering through the mixing zone. In the diffusing zone, the velocity of the refrigerant mixture is reduced causing an intermediate pressure to be achieved. The outlet stream flows into a separator where the vapour and liquid refrigerant are separated with the vapour flowing to the compressor and the liquid flowing through an expansion device before entering the evaporator. With an ejector, the compressor suction pressure is higher for the same evaporation pressure. Therefore an ejector reduces throttling losses and decreases the pressure ratio [39,40,65], which is particularly important for HTTHP cycles since compression efficiency is generally reduced with increasing pressure ratio. Aspects of an ejector system that affect COP include the ejector efficiency, entrainment nozzle throat diameter and outlet diffuser diameter.

2.3. Compression

The thermodynamic inefficiencies associated with the compression process make up a significant fraction of the irreversibility of the overall HP cycle. As a result, advancements that reduce the compression work have a significant impact on COP. The Carnot cycle assumes reversible, adiabatic (and therefore isentropic) compression. The work of compression per mole of refrigerant may be calculated using Eq. (4) [53]:

$$w_{isen} = h_2(P_2, s) - h_1(P_1, s) \cong \frac{RT_1}{1-\gamma}\left[\left(\frac{P_2}{P_1}\right)^{\frac{\gamma-1}{\gamma}} - 1\right] \tag{4}$$

where h_1 is the suction enthalpy, h_2 is the discharge enthalpy, P_1 is the suction pressure, P_2 is the discharge pressure, s is the constant entropy at both the suction and discharge, R is the ideal gas constant, T_1 is the suction temperature, and γ is the ratio of specific heat capacity at constant pressure to specific heat at constant volume. Eq. (4) shows that the work of compression is directly proportional to the suction temperature and is also proportional to the pressure ratio (P_2/P_1) raised to a power that is less than 1.

Real compression processes are irreversible. The efficiency of a compression process (η_{isen}) is evaluated by comparing the work required for isentropic compression (w_{isen}) to that required by the real compression process (w_{shaft}). In addition to the irreversibility of the compression process, the electric motor that runs the compressor has an overall efficiency of the compressor (η_o) resulting from the product of the isentropic efficiency (η_{isen}) and the motor efficiency (η_{motor}),

$$\eta_o = \eta_{isen}\eta_{motor}, \quad \text{where } \eta_{isen} = \frac{w_{isen}}{w_{shaft}},\ \eta_{motor} = \frac{w_{shaft}}{w_{el}} \tag{5}$$

where w_{isen} is the isentropic work, w_{shaft} is the shaft work, and w_{el} is the electricity consumption by the compressor.

The efficiency of the compressor is mainly a function of the pressure ratio and the compressor design. The larger the temperature difference between the heat source and heat sink, the larger the pressure ratio required, and, typically, the lower the compression efficiency [26]. Multi-staging the compression process can reduce the pressure ratio of each compression stage such that each single-stage operates near its maximum isentropic efficiency and increases the overall compression efficiency [54].

Cooling the refrigerant at a constant pressure between compression stages (intercooling) can reduce the work of compression of the higher stage due to a lower average compression temperature; however, the discharge temperature of the higher stage will be reduced, which may not be desirable for HTHP applications, but can help reduce lubricant breakdown.

When a flash vessel is positioned after an initial expansion at an intermediate pressure, the gaseous refrigerant (that is not useful for heat absorption) can be separated from the liquid phase and mixed with the discharge gas from a low-stage compressor and then recompressed. At an intermediate pressure, the compression work will be reduced relative to a single compression stage. In addition, flash gas partially cools the low-stage discharge vapour, which is superheated, such that the high-stage suction vapour is slightly cooler and hence compresses more efficiently. The liquid from the flash tank is expanded to the evaporator pressure having lower volumetric enthalpy than if gas were entrained, thereby reducing the quantity of low-stage expansion flash gas and increasing the enthalpy change during the evaporation process [55]. Alternatively, the low-stage compressor discharge vapour can be directly contacted with intermediate pressure liquid in the flash vessel to fully de-superheat the suction vapour to the high stage compressor (a fraction of the intermediate pressure liquid boils to cool the superheated vapour). In this case, the flash vessel is often called an 'open intercooler'.

Compression performance is also dependent on the refrigerant. Higher suction temperatures tend to decrease the refrigerant density and decrease the volumetric heating capacity meaning the same compressor has a lower mass flow rate, so a larger and more expensive compressor might be required. Another important aspect of the refrigerant is the slope of the isentropes (i.e., lines of constant entropy) on a pressure-enthalpy diagram (Fig. 5b). Conventionally, a low suction temperature and a steep isentrope are desirable to minimise compression work. Some refrigerants may require suction gas superheating to ensure the compression stage does not enter the two-phase region (wet compression, Section 3.1).

In transcritical cycles, optimal discharge pressures are required to maximise the COP of the cycle. Fig. 7 shows a P-h diagram for ammonia with cycles having increasing discharge pressures for a constant process

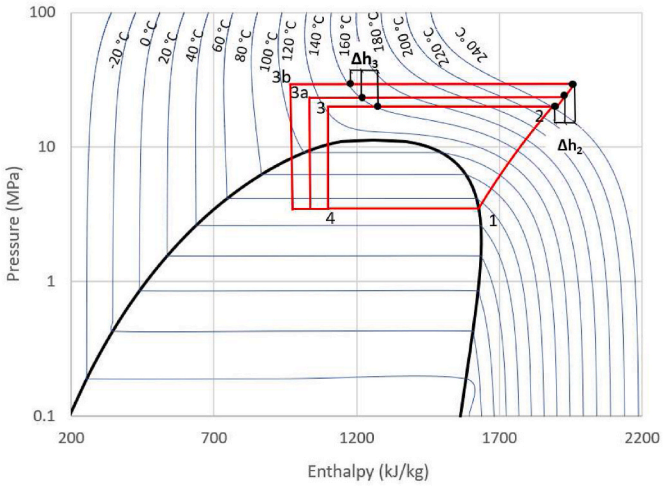

Fig. 7. P-h diagram of transcritical ammonia cycle at different discharge pressures [56].

sink temperature exiting the gas cooler (160 °C) in which the enthalpies of Points 2 and 3 are varied. It can be seen that as the pressure changes, the slopes of the isotherms vary, which changes the properties of the refrigerant throughout the gas cooler [56]. As the discharge pressure increases, the COP for the HP is determined using Eq. (6), which may be used to identify the optimum pressure for achieving maximum COP. The optimum discharge pressure will be a trade-off between increased heating capacity at a higher pressure and higher compression work. The optimum pressure tends to be much larger than the critical pressure because the refrigerant isotherms are very flat (high heat capacity) near the critical point.

$$COP_{HP} = \frac{(h_2 - h_3) + \Delta h_2 + \Delta h_3}{(h_2 - h_1) + \Delta h_2} \quad (6)$$

In some heat pump cycles the refrigerant is either absorbed into a liquid solvent [57] or adsorbed on a solid surface [58] in order that the energy-intensive vapour compression process may be avoided. In the absorption heat pump cycle the refrigerant/absorbent mixture is pumped as a liquid up to a higher pressure where the refrigerant is liberated from the absorbent in a regenerator through the transfer of heat. In adsorption refrigeration no pumping or vapour compression is required as the process is driven entirely by heat [59]. The thermodynamic efficiency of these systems tends to be significantly lower than for vapour compression cycles with COPs often below 1 [60]; however, if waste heat or solar heating is available they may compete economically with vapour compression cycles.

2.4. Condensers, gas coolers and evaporators

A HP cycle requires at least two heat exchangers. As essential components of the cycle, the condenser/gas cooler and evaporator are the connections to the heat sink and heat source streams. Internal heat exchangers (IHXs) can be added to the cycle as an advancement to transfer heat between the refrigerant at different locations within the cycle. The addition of IHXs can improve cycle performance and influence the performance of other components such as the compressor. This advancement is covered in Section 4.

Ipek et al. [61] demonstrated that the optimal operating conditions coupled with the most desirable heat exchanger type will minimise entropy generation (irreversibility) and work. Smaller temperature differences across the heat exchangers, however, generally require larger heat exchangers and greater capital costs. As a result, the design and sizing of the heat exchangers involve the optimisation of the acute trade-off between capital cost and cycle COP. A transcritical cycle could aid in the reduction of heat transfer related losses if the heat sink requires heating over a wide temperature range [62].

Entropy generation, which indicates exergy destruction, in heat exchangers can also occur due to fouling. Fouling is the build-up of foreign material on the heat exchanger surfaces that increases heat transfer resistance [63], which decreases heat exchanger duty and also overall COP. Fouling may be reduced on the refrigerant side of the heat exchanger by employing oil-free compression.

2.5. Refrigerant

The refrigerant choice in a HP impacts its performance, the mechanical design of equipment and its cost. Refrigerant properties that directly affect the COP include the viscosity, thermal conductivity, specific heat capacities (and their ratio), heats of vaporisation, density, critical temperatures, pressures, and volumetric heating capacity. The absolute pressure of the refrigerant within the system should be above atmospheric at every stage such that air and water vapour are not able to enter the system through a leak, and the compressor lubricant should be miscible with the refrigerant. Refrigerant performance is typically related to the proximity of the cycle to the critical temperature and pressure of the refrigerant. For a subcritical cycle, the condensing temperature should be well below the refrigerant's critical temperature to maximise COP. Transcritical cycles, by contrast, involve pressures well above the critical temperature to achieve low gas cooler outlet temperatures to maximise COP. Higher sink temperatures require higher pressures and therefore practical factors such as the maximum pressure ratio can limit the temperatures attainable.

In addition to thermodynamic performance, refrigerant safety and environmental impact are critical factors in refrigerant selection [64]. Refrigerants should preferably be non-toxic and non-flammable. Both chlorofluorocarbons (CFCs) and hydrochlorofluorocarbons (HCFCs) have significant ozone depletion potential (ODP), which has led to the phase-out of chlorine-containing refrigerants in accordance with the Montreal Protocol. Hydrofluorocarbons (HFCs) with zero ODP initially replaced CFC and HCFC refrigerants; however, this comes at the cost of high global warming potential (GWP) [19]. Many countries have aligned with the Kigali Amendment of the Montreal Protocol [65], and the Kyoto Protocol [66] to undergo the eventual phase-out of HFCs.

Significant research into, and development of hydrofluoroolefins (HFOs), hydrochlorofluoroolefins (HCFOs) and natural refrigerants are ongoing as options to replace HFCs. Table 2 shows a list of these common refrigerants (including those of interest with HTHPs), summarising their thermodynamic properties, GWP, ODP and safety index. In the refrigerant safety index, higher numbers correspond to increased flammability (1 = non-flammable, 3 = highly flammable), while the letter 'L' after the number represents a subclass of lower flammability. The letter 'A' refers to low toxicity and 'B' refers to high toxicity. As a result, class A1 represents the safest refrigerant. Table 2 shows how much higher the GWP for HFC refrigerants are compared to the HFOs, HCFOs and natural refrigerants. Carbon dioxide, isopentane and R1336mzz(Z) have very low environmental impacts while also having A1 safety ratings.

Refrigerant blends generate more options for refrigerant selection. Where two refrigerants have different boiling points, temperature glide will occur in the saturation region. The shape and degree of the temperature glide depend on the relative fluid properties and blend composition. Zühlsdorf et al. [43] demonstrated this concept using a blend of dimethyl-ether and CO_2 to obtain a temperature glide that closely paralleled the process heat source and sink requirements, which minimised exergy destruction and maximised COP.

Table 2
Properties of potential high-temperature refrigerant fluids (included in REFPROP [67]).

Refrigerant	Type	P_{crit} (kPa)	T_{crit} (°C)	GWP	ODP	Safety group
R1224yd(Z)	HCFO	3337	155.5	1	minimal	A1
R1233zd(E)	HCFO	3624	166.5	1	minimal	A1
R1234-yf	HFO	3382	94.7	<1	0	A1
R1234ze(E)	HFO	3635	109.4	6	0	A2L
R1234ze(Z)	HFO	3531	150.1	<1	0	A2L
R1243zf	HFO	3518	103.8	<1	0	A2
R1336mzz (Z)	HFO	2903	171.4	2	0	A1
Ammonia	Natural	11,363	132.4	0	0	B2L
CO_2	Natural	7377.3	31.0	1	0	A1
Water	Natural	22,064	374.0	0	0	A1
Propane	Natural	4251.2	96.7	3	0	A3
Isobutane	Natural	3629	134.7	4	0	A3
Butane	Natural	3796	152.0	4	0	A3
Isopentane	Natural	3378	187.2	5	0	A3
Pentane	Natural	3368	196.6	5	0	A3
R245fa	HFC	3651	153.9	1030	0	B1
R365mfc	HFC	3266	186.9	794	0	A2
R410a	HFC	5782	78.1	675	0	A1
R134a	HFC	4059.2	101.1	1430	0	A1
R227ea	HFC	2925	101.8	3220	0	A1

3. Advancements in high-temperature heat pumps

A significant number of studies of HP cycles (experimental and/or simulation-based) that incorporate one or more of the advancements described in Section 3 have been performed. The review identified 49 different cycle configurations found in the literature, along with refrigerant and performance data. Each cycle is presented in the following subsections using a standard set of symbols, which are presented in Fig. 8.

The 49 cycles are overviewed in this section and classified into structural features that are common cycle improvement strategies. Tables 3–9 present the various cycles with a summary of published performance data. The cycles are assigned a code characterised first by transcritical (T) or subcritical (S) operation, followed by the distinctive structural components within the cycle (where applicable). For example, the cycle SE-3 is the third subcritical heat pump cycle identified with an economiser. Where possible, transcritical cycles are numbered corresponding to the structurally equivalent subcritical cycle, i.e., TE-3 is the same cycle as SE-3 except with a gas cooler instead of a condenser. Some subcritical cycles have no transcritical cycle equivalent, which results in numbers being skipped.

3.1. Standard cycle and external subcoolers

A standard HP cycle (Fig. 3a) with a sub-cooler can achieve a high COP for low-temperature lifts. Subcoolers using a separate external heat sink reduce the throttling flash gas and reduce the total refrigerant flow rate for the same heat flow (Table 3 - Cycles S1-1c, S1-2 b). The use of a subcooler maximises COP but depends on the heat demand profile of the process sink.

For standard cycles, the maximum temperature lift is restricted by the pressure ratio limit of a single compression stage. In addition, as temperature lift increases, throttling losses also increase with the extent depending on the refrigerant properties. The maximum temperature lift in a standard cycle with a single compression stage is typically 80 °C with most reported temperature lifts being closer to 30 °C. The more advanced cycles (Sections 3.2 to 3.8) have reported mean temperature lifts of up to 110 °C.

For a range of refrigerants with heat sink temperatures below 100 °C, COPs from 1.8 to 6.6 have been reported. In the heat sink temperature range above 100 °C, COPs between 1.7 and 2.8 have been achieved (Table 3 - Cycles S1-1a,c,d). Multiple standard cycles in parallel (i.e., not a cascade cycle) can improve the COP substantially when the heat sink involves a large temperature glide; e.g., Kondou and Koyama [68] obtained an overall COP of 4.22 for a source temperature of 80 °C with multiple heating stages up to 160 °C.

Many standard HP cycles employ a liquid and vapour separator (Table 3 - Cycle S1-1 b). The separator helps to improve cycle performance by allowing a fully wetted heat transfer surface in the evaporator and minimising the superheat at the compressor while ensuring liquid refrigerant does not enter the compressor. Of the cycles with separators, the heat sink temperatures were all in the high-temperature range (>100 °C) and achieved COPs ranging between 1.9 and 5.5 depending on the source temperature. Standard transcritical CO_2 cycles have achieved COPs between 1.6 and 3.6 (Table 3 - Cycle T1-1).

3.2. Internal heat exchanger

The most common placement for internal heat exchangers (IHX) is between the outlet of the condenser/gas cooler and the outlet of the evaporator [112] (Table 3 - Cycles S1-2a,b and Table 4 - T1-2). When the refrigerant exiting the condenser/gas cooler transfers some heat to the refrigerant exiting the evaporator, the refrigerant temperature at the compressor suction is increased, and hence a higher compressor discharge temperature may be achieved so that the heat sink may reach a higher temperature at the expense of increased compression work (Eq. (4)). There is a range of ways the operation of the IHX can be manipulated to modify the performance of the cycle. Commonly manipulated parameters include the quantity of heat transferred, mean temperature difference in the heat exchanger, heat exchanger placement in the cycle, heat exchanger area, and heat exchanger effectiveness.

The analysis in this section is limited to the effect of IHX for cycles that are either in transcritical operation or are operating with a heat sink above 100 °C. For single-stage subcritical cycles above 100 °C (Table 3 - Cycle S1-2a,b), COPs ranged between 1 and 5.45. For the transcritical single-stage cycles (Table 3 - Cycle T1-2), the COPs ranged between 1.2 and 8 for temperatures below 100 °C, and between 1.2 and 2.8 above 100 °C.

IHX design and performance has been shown to influence the performance of the cycle. Using an experimental CO_2 transcritical cycle

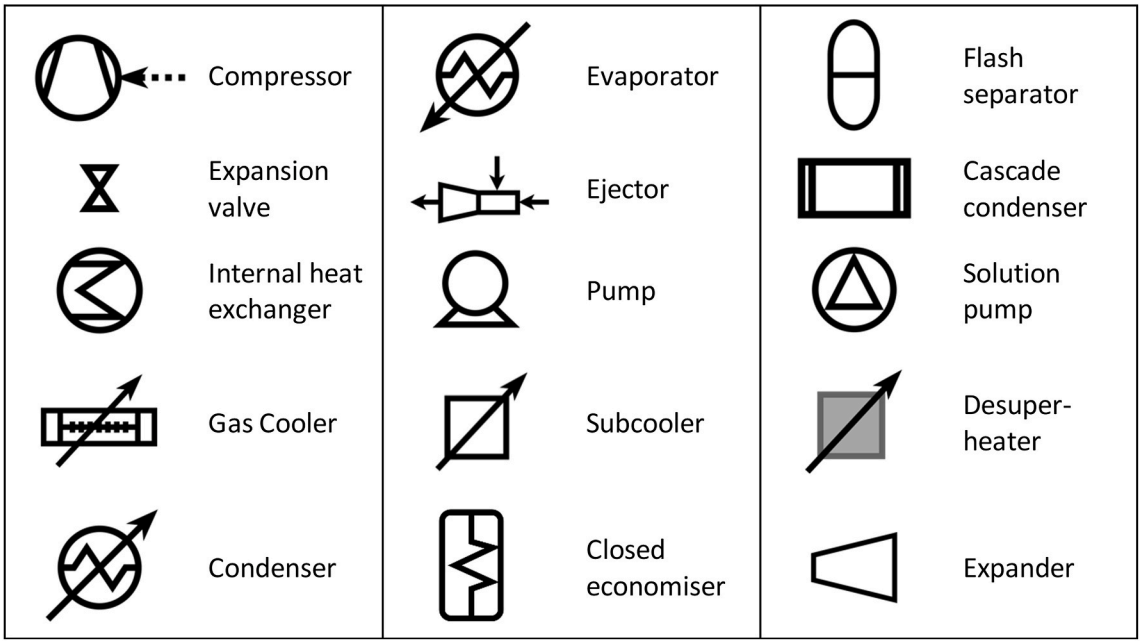

Fig. 8. Key to cycle configuration component symbols used in Tables 3–9.

Table 3
Standard cycle with and without external subcooler.

Code	Cycle schematic and description	$T_{sink\ (out)}/T_{cond}$ (°C)	$T_{source\ (in)}/T_{evap}$ (°C)	ΔT_{LM}	Refrigerant	COP	Experimental (E) or Simulation (S)	Ref.	Year
S1-1a	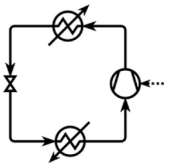 Subcritical, single stage (Standard subcritical vapour compression cycle)	40/-	−10 – 12/-	–	R290	2.6–5	E	[69]	2004
		30/-	11.5/-	20.0	R134a	4.5	E	[70]	2011
		45/-	35/-	–	R142b	4.43	E	[71]	2010
		75/-	45/-	18.9	R1234ze (E)	6.2	E	[72]	2014
		75/-	45/-	18.9	R1234ze (Z)	5.4	E	[72]	2014
		75/-	45/-	18.9	R1234ze (E)	6.2	S	[72]	2014
		75/-	45/-	18.9	R1234ze (Z)	6.6	S	[72]	2014
		65/-	4.6/-	30.3	CO_2	3.1	E	[73]	2016
		124–130/-	80/-	–	BY-5	2.75–2.55	E	[74]	2017
		124–130/-	80/-	–	BY-5	2.775–2.6	S	[74]	2017
		60/-	0/-	–	R152a	2.5	S	[75]	2019
		70/-	0/-	–	R152a	2.1	S	[75]	2019
		80/-	0/-	–	R152a	1.8	S	[75]	2019
		140/-	60–100/-	–	R1234ze (Z)	1.7–3.2	S	[76]	2020
S1-1b	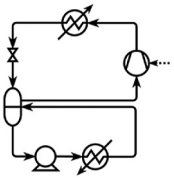 Subcritical, single stage with separator	118–122/-	86–94/-	–	Water	4.8–5.5	E	[77]	2014
		-/120 - 128	-/87	–	Water	5–4.2	S	[78]	2019
		-/121.5–126.3	-/87	–	Water	4.6–4.1	E	[78]	2019
		-/110–150	-/75	–	R718	4–1.9	E	[79]	2020
		-/110–150	-/80	–	R718	4.8–1.9	E	[79]	2020
		-/110–150	-/85	–	R718	6.1–2	E	[79]	2020
S1-1c	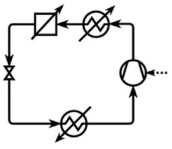 Subcritical, single stage with subcooler	97.3/-	73.9/-	26.8	R245fa	2.4	E	[80]	2016
S1-1d	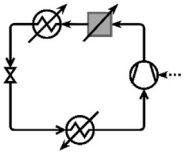 Subcritical, single stage with desuperheater	48/-	- 12–2/-	–	R717	3.8–4.8	E	[81]	2008
T1-1	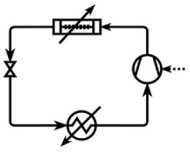 Transcritical, single stage (Standard transcritical vapour compression cycle)	45–70/-	11/- 5	23.0–31.1	CO_2	3.15–2.5	S	[82]	2013
		-/25–30	-/0	–	CO_2	3.45–1.6	S	[83]	2019
		-/25–30	-/0	–	CO_2	3.55–1.65	S	[83]	2019
		57.8/-	10/-	18.8	CO_2	2.8	E	[84]	2010
		27/-	35/-	–	CO_2	1.72	E	[85]	2017
		-/30–50	-/10	–	CO_2	3.25–1.75	E	[86]	2017
		113/-	-/30	–	R134a	3.85	S	[87]	2018
		150/-	82/-	–	R1234ze (Z)	3.32–3.72	E	[88]	2019
		100–200/-	-/20–60	–	CO_2	3.52–1.52	S	[89]	2007
		200/-	30–80/-	–	R601	2.9–3.3	S	[90]	2020
		200/-	30–80/-	–	R514A	2.9–3.3	S	[90]	2020
		200/-	30–80/-	–	R1234ze (Z)	2.9–3.3	S	[90]	2020
		200/-	30–80/-	–	R1233zd (E)	2.9–3.2	S	[90]	2020
		200/-	30–80/-	–	R1224yd (Z)	2.9–3.1	S	[90]	2020
		200/-	30–80/-	–	R245fa	2.9–3.1	S	[90]	2020
		200/-	30–80/-	–	R600	2.9–3.0	S	[90]	2020
S1-2a	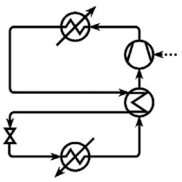 Subcritical, single stage with IHX	160/-	80/-	4.4	R1234ze (Z)	4.24	E	[91]	2017
		160/-	80/-	4.4	R1233zd (E)	4.18	E	[91]	2017
		160/-	80/-	4.4	R365mfc	3.68	E	[91]	2017
		-/105–125	-/25	–	R1233zd (E)	3.2–2.3	E	[52]	2019
		-/105–125	-/25	–	R600	3.1–2.2	E	[52]	2019
		140/-	60–100/-	–		1.7–3.2	S	[76]	2020

(*continued on next page*)

Table 3 (*continued*)

Code	Cycle schematic and description	$T_{sink\ (out)}/T_{cond}$ (°C)	$T_{source\ (in)}/T_{evap}$ (°C)	ΔT_{LM}	Refrigerant	COP	Experimental (E) or Simulation (S)	Ref.	Year
					R1234ze (Z)				
		130/-	30–90/-	–	R245fa	1–5.45	S	[92]	2021
S1-2b	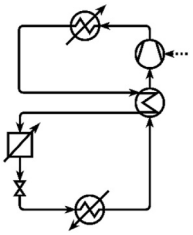	-/120	-/60	–	ECO3	1–2	E	[93]	2012
	Subcritical, single stage with IHX and external sub-cooler								
T1-2	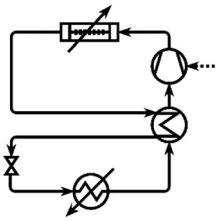	-/35	-/−17	–	CO_2	2.35	S	[94]	2005
		60/-	10/-	–	CO_2	3	E	[95]	2005
		-/120	-/5	–	CO_2	1.2	E	[96]	2008
		45–70/-	−11/−5	23.0–31.1	CO_2	2.85–2.28	E	[82]	2013
		55–80/-	35/-	–	CO_2	4.5–3.5	E	[97]	2013
		55/-	12/0	25.1	CO_2	2.9	E	[98]	2017
		75/-	−20 – 20/-	–	CO_2	2.45–4.4	S	[99]	2018
		10–20/-	10/-	–	CO_2	2.6–2.1	E	[100]	2018
		-/33	20/-	–	CO_2	3.9	E	[101]	2019
		-/25–30	-/0	–	CO_2	3.5–1.7	S	[83]	2019
		70/127.5	7/-	–	CO_2	2.75	S	[102]	2019
		-/40	-/10	–	CO_2	2.9	S	[103]	2000
		37/34	15/-	–	CO_2	3.6	E	[104]	2020
		-/33–45	-/20	–	CO_2	4.75–2.25	E	[105]	2010
		-/33–45	-/20	–	CO_2	8–3.5	S	[105]	2010
		-/25–30	-/0	–	CO_2	3.4–4.7	S	[83]	2019
		100/160	-/0	–	CO_2	2.31	S	[106]	2017
		90/-	−6.4/-	–	CO_2	2.5	S	[107]	2002
		150/-	82/-	–	R1234ze (Z)	3.51	E	[88]	2019
		200/-	30–80/-	–	R601	2.7–3.3	S	[90]	2020
		200/-	30–80/-	–	R514A	2.9–3.5	S	[90]	2020
		200/-	30–80/-	–	R1234ze (Z)	2.9–3.4	S	[90]	2020
		200/-	30–80/-	–	R1233zd (E)	2.9–3.4	S	[90]	2020
		200/-	30–80/-	–	R1224yd (Z)	2.9–3.4	S	[90]	2020
		200/-	30–80/-	–	R245fa	2.9–3.4	S	[90]	2020
		200/-	30–80/-	–	R600	2.9–3.3	S	[90]	2020
		180/-	80/-	–	R600	3.5	E	[108]	2018
		110/-	60/-	–	R600	4.5	E	[109]	2020
		110/-	40/-	–	R600	3.3	E	[109]	2020
		160/-	60/-	–	R600	3.1	E	[109]	2020
T1-3	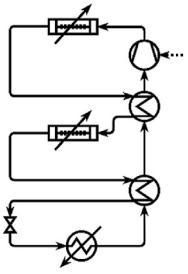	70 & 100/-	-/0	–	CO_2	1.2 (100 °Cwater) + 6.7(70 °C water)3.5	S	[110]	2017
		135/-	5/-	–	CO_2		E	[111]	2019
	Transcritical, single stage with mid-gas cooler IHX and normal IHX								

(Table 3 - Cycle T1-2), Cao et al. [102] observed that an IHX would reduce the discharge pressure while improving COP by around 12%. The optimal discharge pressure was also reduced when introducing an IHX. Similarly, Feng et al. [104] and Zhang et al. [105] also carried out an experimental analysis of transcritical cycles with IHX and emphasised the need for optimising the discharge pressure. Liu et al. [106,110] investigated a transcritical cycle with two IHXs (Table 3 - Cycle T1-3). The first IHX was positioned in between two gas coolers while the second was after the second gas cooler. For their theoretical simulations, the heat pump output was cogeneration of hot water at two temperatures, 71 °C and 100 °C, with a combined heating COP of 7.9. The cycle is noteworthy because it is a unique transcritical cycle configuration with no subcritical equivalent and represents a direction of possible future research for HTTHPs (Section 5.1).

Table 4
Internal heat exchanger and internal economiser cycles.

Code	Cycle schematic and description	$T_{sink\ (out)}$/ T_{cond} (°C)	$T_{source\ (in)}$/ T_{evap} (°C)	ΔT_{LM}	Refrigerant	COP	Experimental (E) or Simulation (S)	Ref.	Year
SE - 1	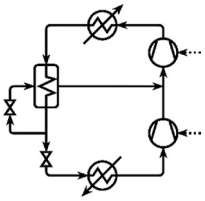 Subcritical, two compression stages with closed economiser	60/- 70/- 80/-	0/- 0/- 0/-	– – –	R152a R152a R152a	2.9 2.5 2.1	S S S	[75] [75] [75]	2019 2019 2019
SE - 2	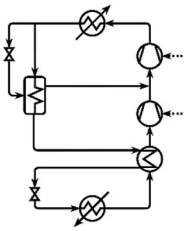 Subcritical, two compression stages with closed economiser and IHX	130/-	30–90/-	–	R245fa	5–2.1	S	[92]	2021
TE-2	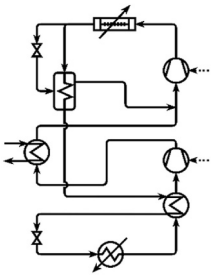 Transcritical, two compression stages with closed economiser, IHX and external intercooling	-/33 30/-	-/2.7 -/−10	– –	CO_2 CO_2	3.25 2.55	S S	[113] [114]	2005 2009
SE - 3	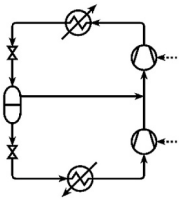 Subcritical, two compression stages with open economiser	127/-	65/-	–	R245fa	3.23	S	[112]	2020
TE-3	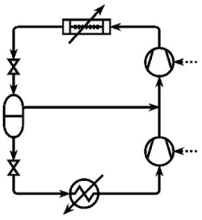 Transcritical, two compression stages with open economiser	60/- 30/- 150/-	5/- 5/- 82/-	– – –	CO_2 CO_2 R1234ze (Z)	1.3 5 3.61	S S E	[115] [115] [88]	2010 2010 2019
SE - 4	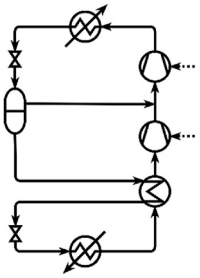 Subcritical, two compression stages with open economiser and IHX	130/- 127/-	30–90/- 65/-	– –	R245fa R245fa	2.5–5 3.651	S S	[92] [112]	2021 2020

(*continued on next page*)

Table 4 (*continued*)

Code	Cycle schematic and description	$T_{sink\ (out)}$/ T_{cond} (°C)	$T_{source\ (in)}$/ T_{evap} (°C)	ΔT_{LM}	Refrigerant	COP	Experimental (E) or Simulation (S)	Ref.	Year
TE-4	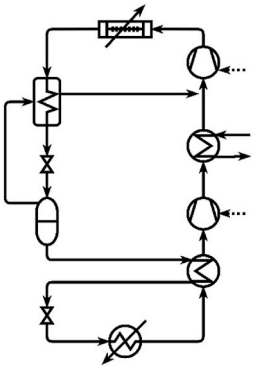 Transcritical, two compression stages with closed and flash economisers, IHX and external intercooling	30/-	-/−10	–	CO_2	2.55	S	[114]	2009
SE - 5	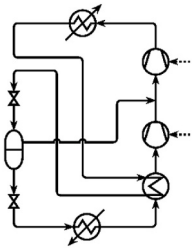 Subcritical, two compression stages with IHX and open economiser	127/-	65/-	–	R245fa	3.59	S	[112]	2020

IHXs are also commonly included in multi-stage (Section 3.3), cascade (Section 3.4), and multi-temperature cycles (Section 3.5). While many studies have shown positive outcomes with the implementation of an IHX, it should also be noted that this is not always the case, particularly from an economic perspective. For HTHPs, this review did not find any study that systematically examines all the variables associated with IHXs that can be manipulated and optimised for COP enhancement; however, this would be a useful direction for future research.

3.3. Internal economiser, intercooling, parallel compression and multi-stage compression

Internal economisers (effectively subcooling via multi-stage expansion) and intercooling are distinct features that can increase COP of a cycle but require additional components, resulting in a trade-off with capital investment. These elements usually require the use of multiple compressors. Parallel compression (or specialised compressors with intermediate pressure economiser ports) enable multi-stage expansion and ensure that the compression of the intermediate flash gas occurs more efficiently at a lower pressure ratio. Multi-stage compression in series has the added advantage of helping maintain compression ratios within optimal ranges and/or enabling multi-temperature heat rejection or multi-stage expansion.

Cycles SE-1,2 (Table 4) both use multi-stage compression and a closed economiser (i.e., heat exchanger) arrangement to supply an intermediate pressure vapour flow for recompression, with the addition of an IHX distinguishing Cycle SE-2 from Cycle SE-1. Cycles SE-3,4,5 (Table 4) apply open (or flash) economisers to produce an intermediate pressure vapour flow. Cycles SE-4,5 also include an IHX with the difference between them being the location of the IHX relative to the flash economiser. COP values varied from 2.1 to 5 for these five cycles. Cycle TE-3 (Table 4) is the transcritical equivalent of Cycle SE-3 (flash economiser, no IHX) while Cycles TE-2,4 (Table 4) are similar to the subcritical Cycles SE-2,4. Studies on these last three transcritical cycles all used CO_2 as the refrigerant and achieved COPs of 1.3–5.

Intercooling is another approach to improve compression efficiency. Cycle SI-1 (Table 5) shows a full subcritical two-stage expansion and compression cycle where an open economiser is used to fully intercool the suction gas (i.e., zero superheat) to the second compression stage. The advantage of full intercooling is to lower the average gas compression temperature. Cycle SI-2 (Table 5) demonstrates direct intercooling within a cycle using an open economiser that is also indirectly heated using a heat exchanger, which enables both better compression efficiency and reduced throttling loss due to subcooling of the high-pressure liquid refrigerant. Cycle SI-3 (Table 5), in contrast, uses an external sink to perform the intercooling (i.e., no reduction in throttling loss). Only Cycle SI-1 (Table 5) has been applied to heating above 100 °C with COPs ranging from 1.65 to 3.8 depending on the temperature lift. In addition to the subcritical cycles, this review identified one transcritical cycle, Cycle TI-3 (Table 3), which follows a similar structure to Cycle SI-3 (except for an IHX). COPs for this cycle were 2.4–2.8.

Parallel compression (Table 5 - Cycle SP-1) enables two-stage expansion with two compressors. The main compressor has gas suction from the evaporator and discharges at the intermediate pressure. A second compressor has gas suction from an intermediate pressure (after the first expansion valve) and discharges at the high pressure. The compressor efficiency is high due to the low-pressure ratio. As a result, the two compressors operate in parallel. Cycles TP1-1 and TP1-2 (Table 5) implement parallel compression in a single “economised” compressor. This reduces compressor cost and has the advantage that in the first expansion stage flash gas is only compressed from the intermediate pressure. However, the compressor efficiency for flash gas compression tends to be lower than full parallel compression due to the

Table 5
Intercooling, parallel compression and multi-stage compression cycles.

Code	Cycle schematic and description	$T_{sink\ (out)}$/ T_{cond} (°C)	$T_{source\ (in)}$/ T_{evap} (°C)	ΔT_{LM}	Refrigerant	COP	Experimental (E) or Simulation (S)	Ref.	Year
SI-1	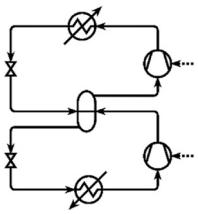 Subcritical, two compression stages with open economiser/intercooler	140/-	40–100/-	–	R1234ze (Z)	1.8–3.8	S	[76]	2020
		150	40	–	R1234ze (Z)	1.65	S	[76]	2020
SI-2	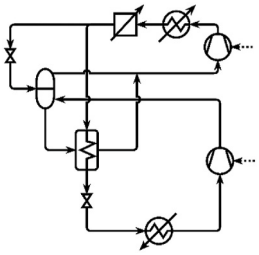 Subcritical, two compression stages with open intercooler, closed economiser and external subcooler	-/77	-/0	–	R717	3.4	S	[106]	2017
SI-3	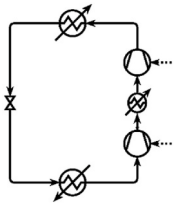 Subcritical, two compression stages with external intercooler	75/-	−20 – 20/-	–	NH_3	3–5.75	S	[99]	2018
TI-3	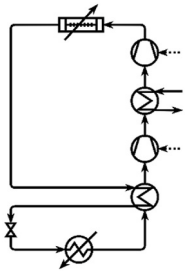 Transcritical, two compression stages with IHX and external intercooling	-/33	-/2.7	–	CO_2	2.82	S	[113]	2005
		30/-	-/−10	–	CO_2	2.37	S	[114]	2009
SP-1	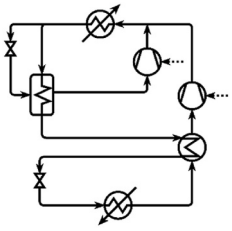 Subcritical, single stage with closed economiser, parallel compression and IHX	130/-	30–90/-	–	R245fa	6.9–1.5	S	[92]	2021
TP-1	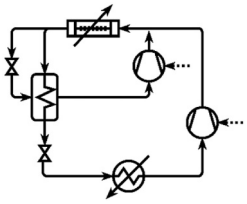 Transcritical, single stage with closed economiser and parallel compression	60/-	5/-	–	CO_2	1.3	S	[115]	2010
		30/-	5/-	–	CO_2	5.05	S	[115]	2010
TP-2		60/-	5/-	–	CO_2	1.3	S	[115]	2010

(*continued on next page*)

Table 5 (*continued*)

Code	Cycle schematic and description	$T_{sink\ (out)}$/ T_{cond} (°C)	$T_{source\ (in)}$/ T_{evap} (°C)	ΔT_{LM}	Refrigerant	COP	Experimental (E) or Simulation (S)	Ref.	Year
	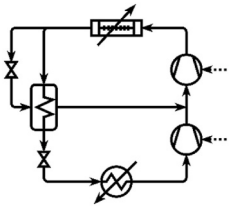 Transcritical, single stage with flash economiser and two stage compression	30/-	5/-	–	CO_2	5.05	S	[115]	2010
TP-3	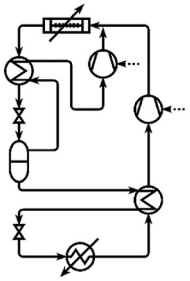 Transcritical, single stage with flash economiser with superheating, parallel compression and a IHX	200/-	30–80/-	–	R601	2.6–3.2	S	[90]	2020
		200/-	30–80/-	–	R514A	2.7–3.5	S	[90]	2020
		200/-	30–80/-	–	R1234ze (Z)	2.8–3.4	S	[90]	2020
		200/-	30–80/-	–	R1233zd (E)	2.7–3.2	S	[90]	2020
		200/-	30–80/-	–	R1224yd (Z)	2.7–3.2	S	[90]	2020
		200/-	30–80/-	–	R245fa	2.7–3.3	S	[90]	2020
		200/-	30–80/-	–	R600	2.7–3.3	S	[90]	2020

high overall pressure ratio for the economised compressor. The high-temperature subcritical cycle, Cycle SP-1 (Table 5), uses an expansion valve with a closed economiser to generate the intermediate-pressure vapour, obtaining COPs of 1.5–6.9 for temperature lifts of 100 °C and 40 °C, respectively. The transcritical CO_2 parallel compression cycles (Table 5 - Cycles TP-1,2) both achieved COPs of 1.3 for a 60 °C gas cooler outlet temperature and 5.05 for a 30 °C gas cooler outlet temperature.

3.4. Cascade

Cascade cycles use a heat exchanger to combine two or more closed HP cycles (usually single-stage) forming a cycle with a low-temperature side (bottom cycle – below the cascade heat exchanger) and a high-temperature side (top cycle – above the cascade heat exchanger). The cascade heat exchanger acts as the evaporator and condenser for the top and bottom cycles respectively [94]. A cascade is thermodynamically similar to a two-stage expansion and compression cycle except for the penalty of the cascade heat exchanger temperature difference. Of the subcritical cascade cycles operating at temperatures below 100 °C, COPs between 2 and 4.4 have been reported (Table 6 - Cycles SS-1a,b). For a cascade with subcritical cycles with IHXs at temperatures above 100 °C (Table 6 - Cycles SS-2), the COPs ranged from 2.5 to 4.9.

Cascade cycles can pair cycles with different refrigerants for the top and bottom cycles. Cycles SS-1a and b (Table 6) were studied by Peng et al. [75] who found the COPs ranged from 2 to 4.4 for temperature lifts of 80 °C–60 °C. Cycles TS-1 and TS-2 (Table 6) cascade a subcritical cycle (bottom) up to a transcritical cycle (top). Yang et al. [116] reported that the cycle could improve temperature matching compared to a single-stage and result in better performance. Cycles TS-1 and TS-2 (Table 6) achieved COPs between 1.95 and 5.24. In Cycle TT-3 (Table 6), both top and bottom cycles are transcritical with the cascade exchanger positioned after the main gas cooler of the bottom cycle, supplying heat to the evaporator of the top cycle. For a specific case, the COP was simulated to be 2.4.

3.5. Multi-temperature

Multi-temperature HP cycles include multiple condensers (or gas coolers) to supply heat to the process sink(s) and/or multiple evaporators to absorb heat from the process source(s). As a result, it is common to customise a multi-temperature cycle to fit a specific application. The use of cascades, internal economisers, intercooling, parallel and multi-stage compression, and IHX can all feature within a cycle to maximise COP. However, there is a natural efficiency-capital trade-off as the number of units within a cycle increases for a diminishing return in COP.

Cycles SM-1 to 5 (Table 7) present various subcritical HTHPs supplying heat sinks above 100 °C. COPs range from 1.2 up to 6.7. For example, Kondou and Koyama [68] analysed advanced, multi-temperature HTHP cycles with three compression stages and various low GWP refrigerants (Table 7 - Cycles SM-4a,b). An additional IHX and condenser stage increased the COP from 4.53 to 4.77 for source and sink temperatures of 80 °C and 160 °C. For similar source and sink temperatures, Fukuda et al. [91] experimentally investigated a cycle with only two compressors, two condensers, one IHX and a subcooler. They tested R1234ze(Z), R1233zd(E) and R365mfc and identified R1234ze(Z) as the refrigerant with the highest COP at 4.58. Cycle TM-6, a partial cascade of two single-stage transcritical cycles, is different to the subcritical multi-temperature cycles and the only transcritical-based cycle (COP of 2.27) identified by the study to include multiple gas coolers that supply heat to the process sink.

3.6. Expander

Transcritical cycles are often able to use conventional expanders instead of expansion valves to recover work if the expansion does not cause the formation of a two-phase fluid (e.g., Table 8 - Cycles TX-1,2). Cycle TX-1 achieved a COP of 2.6 at a high side pressure of 8.6 MPa (45 °C temperature lift) which was a 37.5% increase in COP and 3.9% decrease in pressure compared to a standard cycle. For Cycle TX-2 (Table 8), a COP of 3.3 was achieved at a gas cooler outlet temperature of 35 °C and an evaporation temperature of 0 °C [83].

Table 6
Cascade cycles.

Code	Cycle schematic and description	$T_{sink\ (out)}$/ T_{cond} (°C)	$T_{source\ (in)}$/T_{evap} (°C)	ΔT_{LM}	Refrigerant	COP	Experimental (E) or Simulation (S)	Ref.	Year
SS-1a	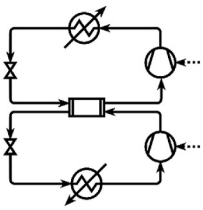 Cascade with sub-critical, single stage (top) and sub-critical, single stage (bottom)	60/-	0/-	–	R152a	2.7	S	[75]	2019
		70/-	0/-	–	R152a	2.3	S	[75]	2019
		80/-	0/-	–	R152a	2	S	[75]	2019
SS-1b	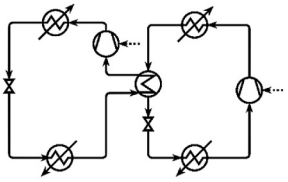 Cascade with sub-critical, single stage (top – left cycle) and sub-critical, single stage (bottom – left cycle) with subcooler (suction superheater for top cycle)	60/-	0/-	–	R717 & R152a	4.4	S	[75]	2019
		70/-	0/-	–	R717 & R152a	3.7	S	[75]	2019
		80/-	0/-	–	R717 & R152a	3.5	S	[75]	2019
TS-1	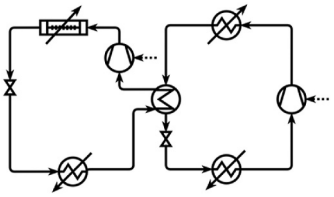 Cascade with transcritical, single stage (top – left cycle) and subcritical, single stage (bottom – right cycle) with subcooler (suction superheater for top cycle)	100/-	50/-	24.7	R1234ze(Z) & CO_2	4.43	S	[117]	2018
		92/35	50/0	–	R152a & CO_2	5.24	S	[116]	2017
SS-2	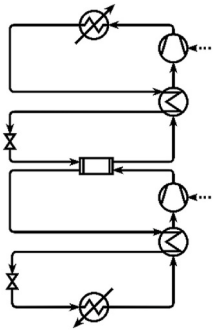 Cascade with subcritical, single stage with IHX (top) and subcritical, single stage with IHX (bottom)	130/-	30–90/-		R245fa	4.9–2.5	S	[92]	2021
TS-2	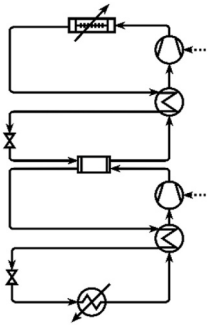 Cascade with transcritical, single stage with IHX (top) and subcritical, single stage with IHX (bottom)	-/35–45	-/−17	–	CO_2	2.7–1.95	S	[94]	2005

(*continued on next page*)

Table 6 (*continued*)

Code	Cycle schematic and description	$T_{sink\ (out)}$/T_{cond} (°C)	$T_{source\ (in)}$/T_{evap} (°C)	ΔT_{LM}	Refrigerant	COP	Experimental (E) or Simulation (S)	Ref.	Year
TT-3	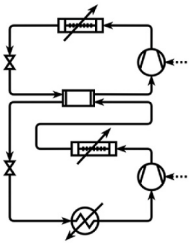 Cascade with transcritical, single stage (top) and transcritical, single stage with gas cooler and cascade in series (bottom)	30/-	-/−10	–	CO_2	2.39	S	[114]	2009

3.7. Ejector

A range of transcritical and subcritical cycles with ejectors have been identified. Cycles S1e-1a,b (Table 8) are subcritical ejector cycles operating below 100 °C that achieved COPs of 4–5.7. Cycles S1e-2,3 (Table 8) are subcritical ejector cycles operating above 100 °C and achieved COPs of 2.4–5.45. Cycles T1e-1,2 (Table 8) are transcritical CO_2 ejector cycles operating below 100 °C with COPs between 1 and 6. Zhu et al. [118], Elbel and Hrnjak [119] and Sun and Ma [120] each analysed a transcritical ejector CO_2 cycle and reported that the addition of an ejector resulted in increases in COP of 10.3%, 7% and 30% increases respectively. To date, no study was found that used ejectors in HTTHP cycles, even though the higher overall compression ratio of a high-temperature cycle would naturally result in improved ejector performance.

As ejector performance is strongly dependant on flow rates and pressures, comparatively small deviations in flow or pressure from design values, such as might occur with varying heat load, can greatly decrease the ejector performance [121]. Variable heat load could be partially addressed using multiple ejectors in parallel, with the number of ejectors in use being proportional to the refrigerant flowrate (heat load). This would allow for the flows through each ejector to remain close to optimal, and for the effect on ejector performance due to variations in the operating conditions to decrease. However, there does not appear to be a simple a solution for the challenge of variable discharge pressure.

3.8. Sorption and hybrid systems

While the majority of sorption cycles have been employed for refrigeration [57], there are some that have been employed for space heating, domestic hot water and even steam generation [127]. A cycle proposed recently was able to produce superheated steam at 180 °C from 80 °C feedwater [128]. In some cases hybrid cycles comprising both sorption and vapour compression processes have been designed [129]. A standard hybrid vapour compression/absorption cycle consists of an absorber, desorber, compressor, solution pump, expansion valve and liquid-vapour separator (Table 9 - Cycle H1-1).

The most common refrigerant combination for absorption-compression hybrid cycles is ammonia and water. Mixing ammonia and water allows for higher heat sink temperatures to occur due to the very high heat of absorption/dissolution for ammonia and water. The solution pump increases the pressure of the water solution, and the compressor increases the pressure of the ammonia vapour. These two streams are then mixed in the absorber where heat is released to the heat sink. Exiting the absorber is the ammonia-rich water solution which is expanded before the desorption process. Ammonia is evaporated in the desorber using heat transfer from the heat source [129]. If the process has more extreme operating conditions and requires more than one equilibrium stage to extract the ammonia from the water, a distillation process could replace the desorber. Though the ammonia concentration decreases throughout the desorption process, the mixture is in the two-phase region for the entirety of the desorption process [130]. Complete evaporation does not occur in the desorber, so a phase separator is required to separate the ammonia vapour from the solution exiting the desorber [130]. Heat transfer occurs over a range of temperatures in both the absorber and desorber, making it convenient to match with high-temperature-glide sinks and sources. The ratio of ammonia to water can also be adapted to align the temperature glide with the heat sink and source temperatures [129].

Passing the mixture through an IHX allows for the temperature of the mixture to decrease before entering the desorber, and to increase before entering the absorber, thereby increasing the overall performance of the cycle [130].

An ammonia-water, subcritical hybrid cycle (Table 9 - Cycle H1-1) operating below 100 °C was presented by Walmsley et al. [131] for a drying application that achieved a COP of 4.5. After the respective compression processes, the water was subcritical, but the ammonia was supercritical when passing through the condenser, hence this cycle is transcritical for ammonia, so the absorber operates in the transcritical region. A COP of around 3.5 is achieved for a top condenser saturation temperature of 55 °C and a 25 °C evaporation temperature. Other subcritical ammonia water hybrid cycles presented in Table 9 are Cycles H1-2 and H1-3 that operate above 100 °C and have COPs ranging from 3 to 4. Ammonia water hybrid cycles show promise for reaching heat sink temperatures above 150 °C.

4. High-temperature transcritical heat pumps

The independence of temperature and pressure in a transcritical cycle gas cooler make it an opportune structure for achieving very high heat sink temperatures for many heating processes; however, HTTHPs are not commonly mentioned in the literature. As seen in Tables 3–8, transcritical HPs are more commonly used in the lower temperature ranges with CO_2 as the refrigerant. However, there are few studies that have investigated transcritical cycles with heat sinks above 100 °C.

A study by Wang et al. [87] analysed the performance of a HTTHP (113 °C) in a drying application. Using a standard transcritical cycle with refrigerant R134a and a subcooler, the drying air was able to reach 113 °C (83 °C temperature lift), at a refrigerant discharge temperature of 125 °C, achieving a COP of 3.85 (Table 3 - Cycle T1-1). Another study of a drying application analysed a standard transcritical cycle (Table 3 - Cycle T1-1) using R1234ze as the refrigerant [88]. From a preheated inlet temperature of 90 °C, the heat sink outlet temperature was able to reach 150 °C with a heat source temperature of 82 °C. The COPs achieved were 3.32–3.72 for air humidity ranging from 160 g_{H2O}/kg_{DA} to

Table 7
Multi-temperature cycles.

Code	Cycle schematic and description	$T_{sink\ (out)}$/ T_{cond} (°C)	$T_{source\ (in)}$/ T_{evap} (°C)	ΔT_{LM}	Refrigerant	COP	Experimental (E) or Simulation (S)	Ref.	Year
SM-1	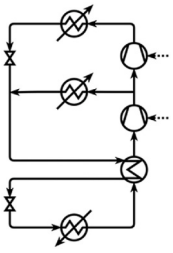 Subcritical, two condenser stages with IHX	130/-	30–90/-	–	R245fa	6.7–1.2	S	[92]	2021
SM-2	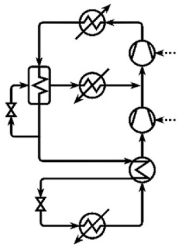 Subcritical, two stage expansion and compression with closed economiser, external superheater and IHX	130/-	30–90/-	–	R245fa	6–1.6	S	[92]	2021
SM-3	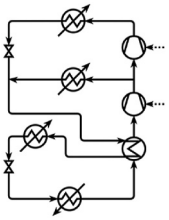 Subcritical, two condenser stages with an IHX and an external subcooler	160/-	80/-	4.4	R1234ze (Z)	4.58	E	[91]	2017
		160/-	80/-	4.4	R1233zd (E)	4.55	E	[91]	2017
		160/-	80/-	4.4	R365mfc	4.44	E	[91]	2017
SM-4a	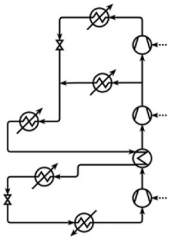 Subcritical, two condenser stages with an IHX and two external subcoolers	160/-	80/-	3.75	R1234ze (Z)	4.53	S	[68]	2015
SM-4b	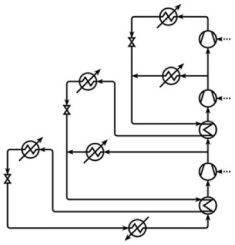 Subcritical, three condenser stages with two IHXs and two external subcoolers	160/-	80/-	3.8	R1234ze (Z)	4.77	S	[68]	2015
SM-5	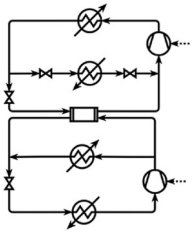 Cascade with subcritical, two evaporator stages (top) and subcritical with parallel condenser stages (bottom)	60/-	0/-	–	R152a	4.5	S	[75]	2019
		70/-	0/-	–	R152a	4	S	[75]	2019
		80/-	0/-	–	R152a	3.6	S	[75]	2019
TM-6		-/45	-/−17	–	CO_2	2.27	S	[94]	2005

(*continued on next page*)

Table 7 (*continued*)

Code	Cycle schematic and description	$T_{sink\ (out)}$/ T_{cond} (°C)	$T_{source\ (in)}$/ T_{evap} (°C)	ΔT_{LM}	Refrigerant	COP	Experimental (E) or Simulation (S)	Ref.	Year
	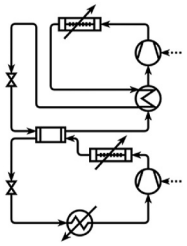 Cascade with transcritical, single stage with IHX (top) and transcritical, series gas cooler and cascade exchanger (bottom)								

200 g_{H2O}/kg_{DA}.

The performance of transcritical cycles (Table 3 - Cycle T1-1) was analysed by Sarkar et al. [89] for heat sink temperatures of up to 200 °C. For a CO_2 cycle, COPs of 3.25, 2.32 and 1.67 were achieved when the heat sink temperature was increased from 30 °C (in all cases) to 100 °C, 150 °C and 200 °C respectively (20 °C heat source temperature). It was concluded that the CO_2 cycle is not appropriate for high temperatures due to the extremely high discharge pressures (as high as 20 MPa). For propane and isobutane transcritical cycles, COPs of 2.59 and 2.65 respectively were achieved when heating to 200 °C.

Wu et al. [117] analysed a transcritical-subcritical cascade system (Table 6 - Cycle TS-1) achieving a heat sink outlet temperature of 100 °C. The subcritical side refrigerant was R1234ze(Z) while the transcritical side used CO_2. At a heat source temperature of 50 °C and a heat sink inlet temperature of 20 °C, a COP of 4.4 was achieved.

Three different cycles to reach heat sink temperatures of 200 °C with a range of refrigerants have been analysed by Arpagaus et al. [90]. These cycles included a standard transcritical cycle (Table 3 - Cycle T1-1), a transcritical cycle with an IHX (Table 3 - Cycle T1-2) and a parallel compression cycle (Table 5 - Cycle TP-3). For their first case study, heat sink temperature increased from 100 °C to 200 °C and heat source temperature decreased from 80 °C to 75 °C. For the standard cycle, R601, R514a, and R1234ze(Z) had the largest COP of 3.3 and corresponding volumetric heating capacities of 2992 kJ/m^3, 3710 kJ/m^3, and 6071 kJ/m^3 respectively. For the cycle with the IHX, the refrigerant with the highest COP at 3.5 was R514a, which had a volumetric heating capacity of 3883 kJ/m^3. R1234ze(Z) had a similar COP (3.4) but a considerably higher volumetric heating capacity at 6187 kJ/m^3. For the parallel compression cycle, a similar result was seen with R514a displaying a COP of 3.5 and a volumetric heating capacity of 3809 kJ/m^3 and R1234ze(Z) displaying a COP of 3.4 and a heating capacity at 6080 kJ/m^3.

White et al. [107], developed a model for a prototype cycle (Table 3 - Cycle T1-2) that was used to analyse operating parameters outside the range of conditions (including temperatures up to 120 °C) that could be experimentally evaluated. According to the model, an increased heat sink temperature caused the optimum discharge pressure to increase while both the COP and heating capacity decreased. At a heat sink temperature of 120 °C (126.4 °C temperature lift), the model predicted a COP of 2.46 and a heating capacity of 60 kW. It also predicted that a 40% increase in the gas cooler heat transfer area would improve both the COP and heating capacity by 5% and 13.5% respectively.

While studies have investigated performances of high-temperature cycles, and transcritical cycles separately, there seem to be few, if any, that have looked at transcritical, high-temperature cycles specifically, particularly for temperatures above 150 °C. Combining the advantages of transcritical cycles with some of the other cycle advancements described above could lead to a new class of HP technology.

5. Critical research challenges and opportunities

The development of new HTTHP technology has significant potential to minimise exergy destruction through further cycle innovations and heat exchange processes that better match heat source and sink profiles. To realise the full potential of this technology, the research community needs to address several challenges relating to HTTHP technology, most of which centre around the compressor.

Challenge 1: Requires the refrigerant to be compressed to extreme pressures, (e.g., >15 MPa for CO_2), making use of current compressor technology difficult. Possible Solution: select or develop cycle structures that intentionally limit the high-pressure requirement through superheating of vapour before compression or use refrigerants with relatively low critical pressures.

Challenge 2: Requires compressors with compression ratios greater than 8, which is higher than the maximum ratios of most current commercial compressors. Possible Solution: apply multiple compression stages to lessen the compression ratio of each stage and place the compression stage in the optimal location within the cycle structure to maximise COP.

Challenge 3: Requires identification of efficient refrigerants (or refrigerant blends), beyond CO_2, to maximise COP for specific applications while keeping within pressure limits. Possible Solution: aim to closely match the refrigerant and process heat load profiles to minimise exergy destruction through the heat transfer processes.

Challenge 4: Needs large heat transfer surfaces for tighter mean temperature differences. Possible Solution: investigate the trade-off between process fluid velocity, which drives the heat transfer coefficient, pressure drop and required pumping power, and cycle temperature lift, which determines the required pressure ratio and compressor power.

Challenge 5: Requires a lubricant that is miscible with the refrigerant and protects and seals the compressor across the full temperature range. Possible Solution: oil-free compressors are becoming more common, but often sacrifice isentropic efficiency.

Challenge 6: Results in high expansion losses due to high compression ratios, generating substantial flash gas and reducing cycle COP. Possible Solution: for some applications, use process integration principles to design a system that cools the supercritical fluid to a sufficiently low temperature that allows for single-phase expansion such that conventional expanders can be used for work recovery.

Each of the possible solutions indicates a need to optimise the integration of the cycle. This includes the selection and arrangement of the components that comprise the cycle and their exchange of heat with the target application. Process integration methodology has traditionally been applied to chemical processes and industrial sites to optimise heat

Table 8
Expander and ejector cycles.

Code	Cycle schematic and description	$T_{sink\ (out)}$/ T_{cond} (°C)	$T_{source\ (in)}$/ T_{evap} (°C)	ΔT_{LM}	Refrigerant	COP	Experimental (E) or Simulation (S)	Ref.	Year
S1e-1a	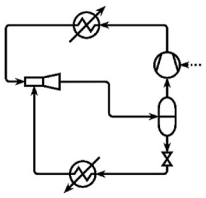 Subcritical, single stage with ejector and separator	-/30	-/−15	–	R12	5.7	S	[122]	1990
		-/35	-/−5	–	R717	4.7	S	[123]	2009
S1e-1b	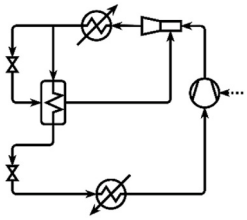 Subcritical, single stage with post-compressor ejector and closed economiser	-/55	-/5		R417A	4	S	[124]	2011
T1e-1	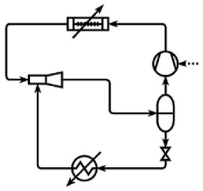 Transcritical, single stage with ejector and separator	-/39–46	-/5	–	CO_2	3–1	S	[120]	2011
		60/-	12/-	–	CO_2	2.75	E	[125]	2017
S1e-2	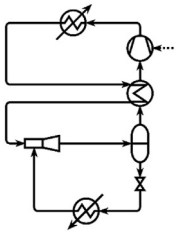 Subcritical, single stage with IHX, ejector and separator	-/105–125	-/25	–	R1233zd (E)	3.5–2.7	E	[52]	2019
		-/105–125	-/25	–	R600	3.5–2.6	E	[52]	2019
		130/-	30–90/-	–	R245fa	1–5.45	S	[92]	2021
T1e-2	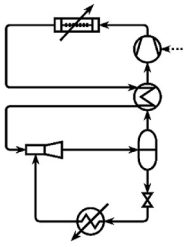 Transcritical, single stage with IHX, ejector and separator	45/-	27/-	–	R744	1.175	E	[119]	2008
		-/40	-/5	–	CO_2	4.5	E	[126]	2003
		-/42	-/0	–	CO_2	1.75	E	[126]	2011
		50–90/-	22/-	–	CO_2	6–3.7	E	[118]	2018
S1e-3	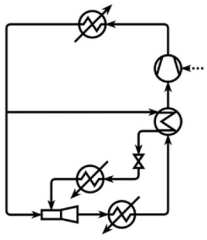 Subcritical, single stage compressor with two evaporator stages, ejector and IHX	-/105–125	-/25	–	R1233zd (E)	3.7–2.6	E	[52]	2019
		-/105–125	-/25	–	R600	3.6–2.4	E	[52]	2019

and mass exchange and minimise utility demand [134]. This methodology can also apply to the development and application of new HP cycles with their target industries. Schlosser et al. [135] introduced one such method to analyse the retrofit potential of both new heat exchangers and HPs using a method called Bridge Analysis.

Table 9
Hybrid cycles.

Code	Cycle schematic and description	$T_{sink\ (out)}/T_{cond}$ (°C)	$T_{source\ (in)}/T_{evap}$ (°C)	ΔT_{LM}	Refrigerant	COP	Experimental (E) or Simulation (S)	Ref.	Year
H1-1	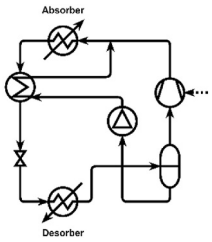 Hybrid, single stage with IHX	87	50	–	NH_3–H_2O	4.5	E	[129]	2011
H1-2	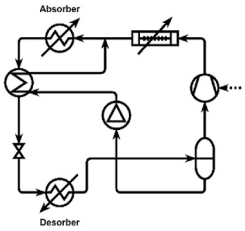 Hybrid, single stage with IHX and gas cooler	111/-	75/-	–	NH_3–H_2O	3–4	S	[132]	2015
H2-1	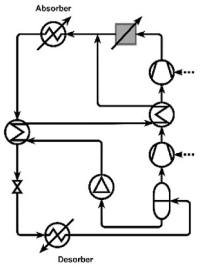 Hybrid, two stage compression with two IHXs	117/-	53/-	–	NH_3–H_2O	3.8	S	[133]	1998

5.1. New cycle with inherently lower maximum pressure requirements

Transcritical CO_2 cycles can output 80 °C–90 °C hot water for industrial and large-scale energy sinks. Increasing the output temperatures above 100 °C encounters constraints around the maximum discharge pressure from a compressor (about 15 MPa for CO_2 cycles). Using Cycles T1-1 or T1-2 (Table 3), a HTTHP cycle would need to reach extreme pressures to obtain the temperatures around 200 °C, which is highly impractical.

The distinguishing feature of a transcritical cycle is that the compressor discharges the refrigerant at a pressure above its critical point. Well beyond the critical pressure, most refrigerants exhibit increasingly linear temperature-enthalpy profiles but have few other benefits. To achieve a target temperature such as 200 °C, two possible processes may be applied – compression or heat exchange. If a HTTHP cycle reaches the maximum pressure ceiling, the balance needs to shift away from compression and more towards heat exchange.

This review proposes two possible ways to shift the critical compression–heat exchange balance. First, external heat from the surrounding process or greater internal heat exchange within the cycle can be applied to superheat the suction gas. The feasibility of using external waste heat in the heat pump is process-specific and can be confirmed using process integration methodology. A concept using internal heat exchange to boost the compressor discharge temperature was presented by Liu et al. [106,110] (Table 3 - Cycle T1-3). Second, a cascade transcritical cycle can be applied where the bottom cycle's gas cooler provides superheat to the suction gas in the top cycle (Fig. 9). This new cascade arrangement could significantly superheat the suction gas, which will reduce the compression required to reach the same discharge temperature. The selection of the optimal combination of refrigerants and operating parameters for the two parts of the cycle is non-trivial and a valuable area of research.

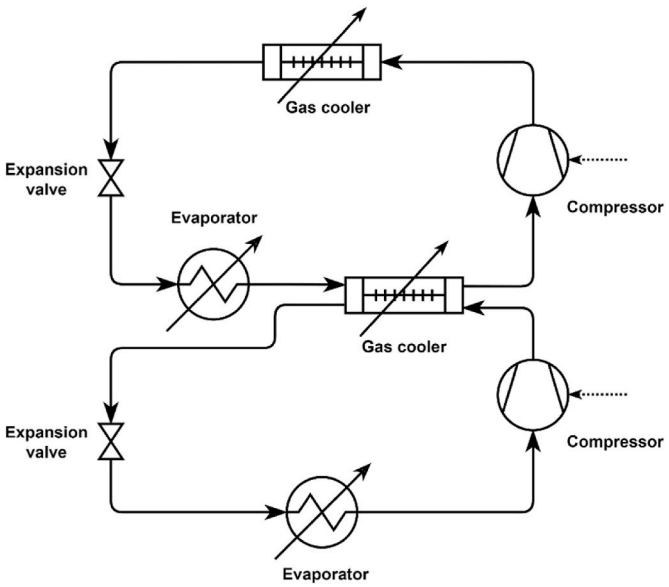

Fig. 9. New transcritical cascade cycle.

5.2. Refining cycle structures to match heat exchange profiles

Townsend and Linnhoff [136] first proposed the concept of appropriate integration of HPs using Pinch Analysis. Pinch Methodology [134] is well known in chemical and process engineering and commonly taught in both undergraduate and postgraduate programmes. A key part of Pinch Analysis is the construction of Composite Curves (heat load profiles of the sources and sinks, separately) and the Grand Composite Curve (a net heat load profile of process sources and sinks). Using the Grand Composite Curve, an engineer can identify "waste" heat below the Pinch Temperature that could be upgraded for heating higher temperature sinks above the Pinch, which is expressed as integration across the Pinch. Non-compliance with this integration rule leads to either: (1) using electricity as a hot utility with an effective system COP of 1 (integration above the Pinch) or (2) an increase in cooling demand with an effective system COP of 0 (integration below the Pinch). The shape and slope of the Grand Composite Curve characterise the heat demand and temperature level requirements of the process. To minimise entropy generation during heat exchange in HPs, the temperature glide of the heat release and absorption profiles should ideally parallel the temperature-load profiles of the background process with a small minimum approach temperature offset (i.e., the Grand Composite Curve).

An avenue to search for new transcritical cycles is through the appropriate placement principles of Pinch Analysis – a key process integration methodology [134]. Fu and Gundersen [137] state that ideally a compressor should be positioned to provide heat above the system Pinch Temperature, i.e., the temperature that divides a region that requires heat (above the Pinch Temperature) and a region that has excess low-grade heat (below the Pinch Temperature). Likewise, an expander is appropriately placed by providing cooling below the Pinch. Using these principles for locating a compressor and expansion in a HP cycle, Fu and Gundersen [138] studied a typical industrial application to recommend a reverse Brayton cycle (also called the Joule cycle) with a single-phase gas refrigerant. Walmsley et al. [131] also applied these principles to a hybrid ammonia-water HP to increase COP. These appropriate placement principles may also be applied to transcritical cycles to lower the maximum pressure requirement.

Many recent studies have identified the suitability of drying processes for the application of HTHPs, especially HTTHPs (e.g. Ref. [87]). For inlet air heating, the gas cooler results in substantial temperature glide as the supercritical fluid cools. On the dryer exhaust side where the evaporator is placed, the exhaust air contains substantial moisture, resulting in substantial latent heat below its dew point. Both the gas cooler and evaporator are well matched to the temperature-load profile of the process, which would minimise exergy destruction and improve COP. This excellent integration solution for drying follows the appropriate application of process integration. Additional industrial applications can similarly be identified using the same approach.

6. Conclusions

A review of HTHP, their advancements, and the potential to associate transcritical cycles with high temperatures (up to 200 °C) and the critical research challenges and opportunities is presented. The paper summarises 49 different existing cycle configurations from the literature with their performance for various temperature ranges and reveals potential outcomes achievable for different HTHP cycle advancements. HPs continue to require research, development, and innovation to stretch the range of applications to ever higher temperatures and temperature lifts. However, continuing with conventional sub-critical cycles will not necessarily unlock the performance gains necessary to make these cycles economic for high temperatures (>100 °C). New transcritical cycles show potential to improve the COP to levels that are competitive with alternative fuels up to temperatures of about 200 °C, operate with feasible pressures, and achieve mean temperature lifts around 100 °C.

Further research is required to explore the capability of HTTHP cycles. Six challenges with corresponding potential solutions have been identified and proposed. This led to the development of a new transcritical cascade cycle concept not seen elsewhere in the literature. Collectively, these challenges and areas provide pathways for future investigation.

Author contributions (Credit statement)

Keri-Marie Adamson: Data curation, Methodology, Investigation, Writing – original draft preparation. **Timothy Gordon Walmsley**: Conceptualization, Methodology, Writing – original draft preparation, Supervision, Funding acquisition, Project administration. **James K. Carson**: Conceptualization, Writing - Reviewing and Editing, Visualization, Funding acquisition. **Qun Chen**: Visualization, Writing - Reviewing and Editing, Funding acquisition. **Florian Schlosser**: Visualization, Writing – original draft preparation. **Lana Kong**: Writing - Reviewing and Editing, Visualization. **Donald J. Cleland**: Conceptualization, Writing - Reviewing and Editing, Funding acquisition.

Declaration of competing interest

The authors declare that they have no known competing financial interests or personal relationships that could have appeared to influence the work reported in this paper.

Data availability

No data was used for the research described in the article.

Acknowledgments

This research has been supported by the programme "Ahuora: Delivering sustainable industry through smart process heat decarbonisation", an Advanced Energy Technology Platform, funded by the New Zealand Ministry of Business, Innovation and Employment.

References

[1] Ritchie H, Roser M. Energy. Our world in data. 2021. https://ourworldindata.org/energy. [Accessed 23 July 2021]. accessed.
[2] Key IEA. World energy statistics 2021. IEA; 2021. https://www.iea.org/reports/key-world-energy-statistics-2021. [Accessed 29 October 2021]. accessed.
[3] Rehfeldt M, Fleiter T, Toro F. A bottom-up estimation of the heating and cooling demand in European industry. Energy Efficiency 2017. https://doi.org/10.1007/s12053-017-9571-y. 1057–82.
[4] Greenhouse IEA. Gas emissions from energy. IEA; 2021. https://www.iea.org/reports/greenhouse-gas-emissions-from-energy-overview. [Accessed 15 December 2021]. accessed.
[5] Cozzi L, Gül T, Bouckaert S, Pales AF, McGlade C, Remme U, et al. Net zero by 2050 - a roadmap for the global energy sector. Paris, France: International Energy Agency; 2021.
[6] Kim J-K, Son H, Yun S. Heat integration of power-to-heat technologies: case studies on heat recovery systems subject to electrified heating. J Clean Prod 2022; 331:130002. https://doi.org/10.1016/j.jclepro.2021.130002.
[7] Jesper M, Schlosser F, Pag F, Walmsley TG, Schmitt B, Vajen K. Large-scale heat pumps: uptake and performance modelling of market-available devices. Renew Sustain Energy Rev 2021;137:110646. https://doi.org/10.1016/j.rser.2020.110646.
[8] Zhu H, Goh HH, Zhang D, Ahmad T, Liu H, Wang S, et al. Key technologies for smart energy systems: recent developments, challenges, and research opportunities in the context of carbon neutrality. J Clean Prod 2022;331:129809. https://doi.org/10.1016/j.jclepro.2021.129809.
[9] Worrell E, Boyd G. Bottom-up estimates of deep decarbonization of U.S. manufacturing in 2050. J Clean Prod 2022;330:129758. https://doi.org/10.1016/j.jclepro.2021.129758.
[10] Wu D, Hu B, Wang RZ. Vapor compression heat pumps with pure Low-GWP refrigerants. Renew Sustain Energy Rev 2021;138:110571. https://doi.org/10.1016/j.rser.2020.110571.
[11] Lund R, Ilic DD, Trygg L. Socioeconomic potential for introducing large-scale heat pumps in district heating in Denmark. J Clean Prod 2016;139:219–29. https://doi.org/10.1016/j.jclepro.2016.07.135.

[12] Zhang J, Zhang H-H, He Y-L, Tao W-Q. A comprehensive review on advances and applications of industrial heat pumps based on the practices in China. Appl Energy 2016;178:800–25. https://doi.org/10.1016/j.apenergy.2016.06.049.

[13] Cao Z, Han X, Lyons W, O'Rourke F. Energy management optimisation using a combined Long Short-Term Memory recurrent neural network – particle Swarm Optimisation model. J Clean Prod 2021;326:129246. https://doi.org/10.1016/j.jclepro.2021.129246.

[14] Haikarainen C, Pettersson F, Saxén H. Optimising the regional mix of intermittent and flexible energy technologies. J Clean Prod 2019;219:508–17. https://doi.org/10.1016/j.jclepro.2019.02.103.

[15] Wang J, Dong F, Ma Z, Chen H, Yan R. Multi-objective optimization with thermodynamic analysis of an integrated energy system based on biomass and solar energies. J Clean Prod 2021;324:129257. https://doi.org/10.1016/j.jclepro.2021.129257.

[16] Koşan M, Aktaş M. Experimental investigation of a novel thermal energy storage unit in the heat pump system. J Clean Prod 2021;311:127607. https://doi.org/10.1016/j.jclepro.2021.127607.

[17] Arpagaus C, Bless F, Uhlmann M, Schiffmann J, Bertsch SS. High temperature heat pumps: market overview, state of the art, research status, refrigerants, and application potentials. Energy 2018;152:985–1010. https://doi.org/10.1016/j.energy.2018.03.166.

[18] Bobelin D, Bourig DA, Peureux J-L. Experimental results of a newly developed very high temperature industrial heat pump (140°C) equipped with scroll compressors and working with a new blend refrigerant. In: International refrigeration and Air Conditioning Conference; 2012. Paper 1299, http://docs.lib.purdue.edu/iracc/1299.

[19] Brodribb P. Hydrofluorocarbon consumption in New Zealand. Expert group; 2017.

[20] Sarkar J. Ejector enhanced vapor compression refrigeration and heat pump systems—a review - ScienceDirect. Renew Sustain Energy Rev 2012;16:6647–59.

[21] Wu D, Hu B, Wang RZ. Vapor compression heat pumps with pure Low-GWP refrigerants. Renew Sustain Energy Rev 2021;138:110571. https://doi.org/10.1016/j.rser.2020.110571.

[22] Chua KJ, Chou SK, Yang WM. Advances in heat pump systems: a review. Appl Energy 2010;87:3611–24. https://doi.org/10.1016/j.apenergy.2010.06.014.

[23] Schlosser F, Arpagaus C, Walmsley TG. Heat pump integration by Pinch analysis for industrial applications: a review, vol. 76; 2019. p. 7–12. https://doi.org/10.3303/CET1976002. 1.

[24] Arpagaus C, Bless F, Schiffmann J, Bertsch SS. Multi-temperature heat pumps: a literature review. Int J Refrig 2016;69:437–65. https://doi.org/10.1016/j.ijrefrig.2016.05.014.

[25] Bamigbetan O, Eikevik TM, Nekså P, Bantle M. Review of vapour compression heat pumps for high temperature heating using natural working fluids. Int J Refrig 2017;80:197–211. https://doi.org/10.1016/j.ijrefrig.2017.04.021.

[26] Gaur AS, Fitiwi DZ, Curtis J. Heat pumps and our low-carbon future: a comprehensive review. Energy Res Social Sci 2021;71:101764. https://doi.org/10.1016/j.erss.2020.101764.

[27] Goyal A, Staedter MA, Garimella S. A review of control methodologies for vapor compression and absorption heat pumps. Int J Refrig 2019;97:1–20. https://doi.org/10.1016/j.ijrefrig.2018.08.026.

[28] Ma Y, Liu Z, Tian H. A review of transcritical carbon dioxide heat pump and refrigeration cycles. Energy 2013;55:156–72. https://doi.org/10.1016/j.energy.2013.03.030.

[29] Fischer D, Madani H. On heat pumps in smart grids: a review. Renew Sustain Energy Rev 2017;70:342–57. https://doi.org/10.1016/j.rser.2016.11.182.

[30] Sarbu I. A review on substitution strategy of non-ecological refrigerants from vapour compression-based refrigeration, air-conditioning and heat pump systems. Int J Refrig 2014;46:123–41. https://doi.org/10.1016/j.ijrefrig.2014.04.023.

[31] Cao F, Song Y, Li M. Review on development of air source transcritical CO2 heat pump systems using direct-heated type and recirculating-heated type. Int J Refrig 2019;104:455–75. https://doi.org/10.1016/j.ijrefrig.2018.12.023.

[32] Lecompte S, Ntavou E, Tchanche B, Kosmadakis G, Pillai A, Manolakos D, et al. Review of experimental research on supercritical and transcritical thermodynamic cycles designed for heat recovery application. Appl Sci 2019;9. https://doi.org/10.3390/app9122571. Switzerland.

[33] Huang F, Zheng J, Baleynaud JM, Lu J. Heat recovery potentials and technologies in industrial zones. J Energy Inst 2017;90:951–61. https://doi.org/10.1016/j.joei.2016.07.012.

[34] Menon A, Stojceska V, Tassou SA. A systematic review on the recent advances of the energy efficiency improvements in non-conventional food drying technologies. Trends Food Sci Technol 2020;100:67–76. https://doi.org/10.1016/j.tifs.2020.03.014.

[35] Mohanraj M, Muraleedharan C, Jayaraj S. A review on recent developments in new refrigerant mixtures for vapour compression-based refrigeration, air-conditioning and heat pump units. Int J Energy Res 2011;35:647–69. https://doi.org/10.1002/er.1736.

[36] Austin BT, Sumathy K. Transcritical carbon dioxide heat pump systems: a review. Renew Sustain Energy Rev 2011;15:4013–29. https://doi.org/10.1016/j.rser.2011.07.021.

[37] Schlosser F, Jesper M, Vogelsang J, Walmsley TG, Arpagaus C, Hesselbach J. Large-scale heat pumps: applications, performance, economic feasibility and industrial integration. Renew Sustain Energy Rev 2020;133:110219. https://doi.org/10.1016/j.rser.2020.110219.

[38] Jiang J, Hu B, Wang RZ, Deng N, Cao F, Wang C-C. A review and perspective on industry high-temperature heat pumps. Renew Sustain Energy Rev 2022;161:112106. https://doi.org/10.1016/j.rser.2022.112106.

[39] Eisa MAR, Best R, Holland FA. Open and closed-cycle mechanical vapour-compression heat-pump assisted sea-water purification systems. Appl Energy 1987;27:203–28. https://doi.org/10.1016/0306-2619(87)90027-4.

[40] Borgnakke C, Sonntag RE. Fundamentals of thermodynamics. tenth ed. New York, USA: Wiley & Sons; 2020.

[41] Çengel YA, Michael AB. Thermodynamics - an engineering approach. seventh ed. Boston, Massachusetts: McGraw-Hill; 2001.

[42] Domanski PA. Minimizing throttling loss in the refrigeration cycle. National Institute of Standards and Technology; 1995.

[43] Zühlsdorf B, Jensen JK, Cignitti S, Madsen C, Elmegaard B. Analysis of temperature glide matching of heat pumps with zeotropic working fluid mixtures for different temperature glides. Energy 2018;153:650–60. https://doi.org/10.1016/j.energy.2018.04.048.

[44] Shatalov IK, Antipov YuA, Dubentsov KG. Use of the Lorenz cycle in heat pumps. Chem Petrol Eng 2018;53:716–9. https://doi.org/10.1007/s10556-018-0410-6.

[45] Zhang Z, Feng X, Tian D, Yang J, Chang L. Progress in ejector-expansion vapor compression refrigeration and heat pump systems. Energy Convers Manag 2020;207:112529. https://doi.org/10.1016/j.enconman.2020.112529.

[46] Pottker G, Hrnjak P. Experimental investigation of the effect of condenser subcooling in R134a and R1234yf air-conditioning systems with and without internal heat exchanger. Int J Refrig 2015;50:104–13. https://doi.org/10.1016/j.ijrefrig.2014.10.023.

[47] Yap KS, Ooi KT, Chakraborty A. Analysis of the novel cross vane expander-compressor: mathematical modelling and experimental study. Energy 2018;145:626–37. https://doi.org/10.1016/j.energy.2017.12.097.

[48] Singh S, Singh A, Dasgupta MS. CFD modeling of a scroll work recovery expander for trans-critical CO 2 refrigeration system. Energy Proc 2017;109:146–52. https://doi.org/10.1016/j.egypro.2017.03.081.

[49] Galoppi G, Secchi R, Ferrari L, Ferrara G, Karellas S, Fiaschi D. Radial piston expander as a throttling valve in a heat pump: focus on the 2-phase expansion. Int J Refrig 2017;82:273–82. https://doi.org/10.1016/j.ijrefrig.2017.06.025.

[50] Zhao L, Li M, Ma Y, Liu Z, Zhang Z. Simulation analysis of a two-rolling piston expander replacing a throttling valve in a refrigeration and heat pump system. Appl Therm Eng 2014;66:383–94. https://doi.org/10.1016/j.applthermaleng.2014.01.055.

[51] Zhang Z, Li M, Ma Y, Gong X. Experimental investigation on a turbo expander substituted for throttle valve in the subcritical refrigeration system. Energy 2015;79:195–202. https://doi.org/10.1016/j.energy.2014.11.007.

[52] Bai T, Yan G, Yu J. Thermodynamic assessment of a condenser outlet split ejector-based high temperature heat pump cycle using various low GWP refrigerants. Energy 2019;179:850–62. https://doi.org/10.1016/j.energy.2019.04.191.

[53] Smith JM, Van Ness HC, Abbott MM. Introduction to chemical engineering thermodynamics. seventh ed. New York: McGraw-Hill; 2005.

[54] Biao X, Tongyi H, Lin H, Yan Y, Yuying S, Wei W. Experimental study of an improved air-source heat pump system with a novel three-cylinder two-stage variable volume ratio rotary compressor. Int J Refrig 2019;100:343–53. https://doi.org/10.1016/j.ijrefrig.2018.11.026.

[55] Hu B, Wu D, Wang LW, Wang RZ. Exergy analysis of R1234ze(Z) as high temperature heat pump working fluid with multi-stage compression. Front Energy 2017;11:493–502. https://doi.org/10.1007/s11708-017-0510-6.

[56] Hu B, He Y, Wang S, Cao F, Xing Z. Field evaluation for air-source transcritical CO2 heat pump water heater with optimal pressure control. In: International refrigeration and Air Conditioning Conference; 2014.

[57] Wu W, Wang B, Shi W, Li X. An overview of ammonia-based absorption chillers and heat pumps. Renew Sustain Energy Rev 2014;31:681–707. https://doi.org/10.1016/j.rser.2013.12.021.

[58] Vasiliev LL, Mishkinis DA, Antukh AA, Vasiliev LL. Solar–gas solid sorption heat pump. Appl Therm Eng 2001;21:573–83. https://doi.org/10.1016/S1359-4311(00)00069-7.

[59] Demir H, Mobedi M, Ülkü S. A review on adsorption heat pump: problems and solutions. Renew Sustain Energy Rev 2008;12:2381–403. https://doi.org/10.1016/j.rser.2007.06.005.

[60] Wang RZ, Oliveira RG. Adsorption refrigeration—an efficient way to make good use of waste heat and solar energy. Prog Energy Combust Sci 2006;32:424–58. https://doi.org/10.1016/j.pecs.2006.01.002.

[61] İpek O, Kılıç B, Gürel B. Experimental investigation of exergy loss analysis in newly designed compact heat exchangers. Energy 2017;124:330–5. https://doi.org/10.1016/j.energy.2017.02.061.

[62] SWEP. 7. 1 General function and theory. SWEP; 2018. https://www.swep.net/refrigerant-handbook/7.-condensers/asd5/. [Accessed 31 August 2021]. accessed.

[63] Oon CS, Kazi SN, Hakimin MA, Abdelrazek AH, Mallah AR, Low FW, et al. Heat transfer and fouling deposition investigation on the titanium coated heat exchanger surface. Powder Technol 2020;373:671–80. https://doi.org/10.1016/j.powtec.2020.07.010.

[64] Longo GA, Zilio C, Righetti G, Brown JS. Experimental assessment of the low GWP refrigerant HFO-1234ze(Z) for high temperature heat pumps. Exp Therm Fluid Sci 2014;57:293–300. https://doi.org/10.1016/j.expthermflusci.2014.05.004.

[65] Environment Committee. International treaty examination of the amendment to the montreal Protocol on substances that deplete the ozone layer. New Zealand: Environment Committee; 2018.

[66] United Nations. Kyoto Protocol. Kyoto, Japan: United Nations; 1997.

[67] Lemmon EW, Huber ML, McLinden MO. NIST standard reference database 23: reference fluid thermodynamic and transport properties-REFPROP. Gaithersburg: National Institute of Standards and Technology; 2018.

[68] Kondou C, Koyama S. Thermodynamic assessment of high-temperature heat pumps using Low-GWP HFO refrigerants for heat recovery. Int J Refrig 2015;53:126–41. https://doi.org/10.1016/j.ijrefrig.2014.09.018.
[69] Fernando P, Palm B, Lundqvist P, Granryd E. Propane heat pump with low refrigerant charge: design and laboratory tests. Int J Refrig 2004;27:761–73. https://doi.org/10.1016/j.ijrefrig.2004.06.012.
[70] Fatouh M, Elgendy E. Experimental investigation of a vapor compression heat pump used for cooling and heating applications. Energy 2011;36:2788–95. https://doi.org/10.1016/j.energy.2011.02.019.
[71] Song Y, Yang W, Wang Z, Xiang X. Indoor analogue tests for high temperature heat pump and its industrial application. In: 2010 International Conference on Future Power and Energy Engineering; 2010. p. 28–33. https://doi.org/10.1109/ICFPEE.2010.15.
[72] Fukuda S, Kondou C, Takata N, Koyama S. Low GWP refrigerants R1234ze(E) and R1234ze(Z) for high temperature heat pumps. Int J Refrig 2014;40:161–73. https://doi.org/10.1016/j.ijrefrig.2013.10.014.
[73] Saikawa M, Koyama S. Thermodynamic analysis of vapor compression heat pump cycle for tap water heating and development of CO2 heat pump water heater for residential use. Appl Therm Eng 2016;106:1236–43. https://doi.org/10.1016/j.applthermaleng.2016.06.105.
[74] Zhang Y, Zhang Y, Yu X, Guo J, Deng N, Dong S, et al. Analysis of a high temperature heat pump using BY-5 as refrigerant. Appl Therm Eng 2017;127:1461–8. https://doi.org/10.1016/j.applthermaleng.2017.08.072.
[75] Peng Z-R, Wang G-B, Zhang X-R. Thermodynamic analysis of novel heat pump cycles for drying process with large temperature lift. Int J Energy Res 2019;43:3201–22. https://doi.org/10.1002/er.4394.
[76] Kosmadakis G, Arpagaus C, Neofytou P, Bertsch S. Techno-economic analysis of high-temperature heat pumps with low-global warming potential refrigerants for upgrading waste heat up to 150 °C. Energy Convers Manag 2020;226:113488. https://doi.org/10.1016/j.enconman.2020.113488.
[77] Chamoun M, Rulliere R, Haberschill P, Peureux J-L. Experimental and numerical investigations of a new high temperature heat pump for industrial heat recovery using water as refrigerant. Int J Refrig 2014;44:177–88. https://doi.org/10.1016/j.ijrefrig.2014.04.019.
[78] Wu D, Yan H, Hu B, Wang RZ. Modeling and simulation on a water vapor high temperature heat pump system. Energy 2019;168:1063–72. https://doi.org/10.1016/j.energy.2018.11.113.
[79] Wu D, Jiang J, Hu B, Wang RZ. Experimental investigation on the performance of a very high temperature heat pump with water refrigerant. Energy 2020;190:116427. https://doi.org/10.1016/j.energy.2019.116427.
[80] Wu X, Xing Z, He Z, Wang X, Chen W. Performance evaluation of a capacity-regulated high temperature heat pump for waste heat recovery in dyeing industry. Appl Therm Eng 2016;93:1193–201. https://doi.org/10.1016/j.applthermaleng.2015.10.075.
[81] Palm B. Ammonia in low capacity refrigeration and heat pump systems. Int J Refrig 2008;31:709–15. https://doi.org/10.1016/j.ijrefrig.2007.12.006.
[82] Jiang Y, Ma Y, Li M, Fu L. An experimental study of trans-critical CO2 water–water heat pump using compact tube-in-tube heat exchangers. Energy Convers Manag 2013;76:92–100. https://doi.org/10.1016/j.enconman.2013.07.031.
[83] Pérez-García V, Belman-Flores JM, Navarro-Esbrí J, Rubio-Maya C. Comparative study of transcritical vapor compression configurations using CO2 as refrigeration mode base on simulation. Appl Therm Eng 2013;51:1038–46. https://doi.org/10.1016/j.applthermaleng.2012.10.018.
[84] Fernandez N, Hwang Y, Radermacher R. Comparison of CO2 heat pump water heater performance with baseline cycle and two high COP cycles. Int J Refrig 2010;33:635–44. https://doi.org/10.1016/j.ijrefrig.2009.12.008.
[85] Song Y, Wang J, Cao F, Shu P, Wang X. Experimental investigation on a capillary tube based transcritical CO2 heat pump system. Appl Therm Eng 2017;112:184–9. https://doi.org/10.1016/j.applthermaleng.2016.10.033.
[86] Song Y, Wang J, Cao F, Shu P, Wang X. Investigation on the adaptivity of the transcritical CO2 refrigeration system with a capillary. Int J Refrig 2017;79:183–95. https://doi.org/10.1016/j.ijrefrig.2017.04.013.
[87] Wang JF, Brown C, Cleland DJ. Heat pump heat recovery options for food industry dryers. Int J Refrig 2018;86:48–55. https://doi.org/10.1016/j.ijrefrig.2017.11.028.
[88] Chahla GA, Beucher Y, Zoughaib A, Carlan FD, Pierucci J. Transcritical industrial heat pump using HFO's for up to 150°C hot air supply, vol. 8; 2019. https://doi.org/10.18462/iir.icr.2019.1184.
[89] Sarkar J, Bhattacharyya S, Ram Gopal M. Natural refrigerant-based subcritical and transcritical cycles for high temperature heating. Int J Refrig 2007;30:3–10. https://doi.org/10.1016/j.ijrefrig.2006.03.008.
[90] Arpagaus C, Bless F, Bertsch SS. Theoretical analysis of transcritical HTHP cycles with low GWP HFO refrigerants and hydrocarbons for process heat up to 200 °C. In: IIR Rankine Conference 2020; 2020. p. 116. https://doi.org/10.18462/iir.rankine.2020.1168.
[91] Fukuda S, Kondou C, Takata N, Koyama S. Thermodynamic analysis on high temperature heat pump cycles using low-GWP refrigerants for heat recovery. Heat Pump Conference 2017;7.
[92] Mateu-Royo C, Arpagaus C, Mota-Babiloni A, Navarro-Esbrí J, Bertsch SS. Advanced high temperature heat pump configurations using low GWP refrigerants for industrial waste heat recovery: a comprehensive study. Energy Convers Manag 2021;229:113752. https://doi.org/10.1016/j.enconman.2020.113752.
[93] Bobelin D, Bourig DA, Peureux J-L. Experimental results of a newly developed very high temperature industrial heat pump (140°C) equipped with scroll compressors and working with a new blend refrigerant. International Refrigeration and Air Conditioning Conference 2012:11.
[94] Liang Y, Yusheng H, Qifan W, Xuetao L. Comparative study of upgraded CO2 transcritical air source heat pump systems with different heat sinks. Appl Therm Eng 2021;184:116289. https://doi.org/10.1016/j.applthermaleng.2020.116289.
[95] Kim SG, Kim YJ, Lee G, Kim MS. The performance of a transcritical CO2 cycle with an internal heat exchanger for hot water heating. Int J Refrig 2005;28:1064–72. https://doi.org/10.1016/j.ijrefrig.2005.03.004.
[96] Aprea C, Maiorino A. An experimental evaluation of the transcritical CO2 refrigerator performances using an internal heat exchanger. Int J Refrig 2008;31:1006–11. https://doi.org/10.1016/j.ijrefrig.2007.12.016.
[97] Wang S, Tuo H, Cao F, Xing Z. Experimental investigation on air-source transcritical CO2 heat pump water heater system at a fixed water inlet temperature. Int J Refrig 2013;36:701–16. https://doi.org/10.1016/j.ijrefrig.2012.10.011.
[98] Sun Z, Liu S, Liang Y, Song M, Guo J. The optimal charge of carbon dioxide in water–water heat pump systems with and without an internal heat exchanger. Trans Hong Kong Inst Eng 2017;24:99–106. https://doi.org/10.1080/1023697X.2017.1317039.
[99] Ivanovski I, Goričanec D, Salamunić JJ, Žagar T. The comparison between two high-temperature heat-pumps for the production of sanitary water. Strojniski Vestnik/J Mech Eng 2018;64:437–42. https://doi.org/10.5545/sv-jme.2017.5082.
[100] Wang D, Yu B, Hu J, Chen L, Shi J, Chen J. Heating performance characteristics of CO2 heat pump system for electrical vehicle in a cold climate. Int J Refrig 2018;85:27–41. https://doi.org/10.1016/j.ijrefrig.2017.09.009.
[101] Yang L-X, Wei X-L, Zhao L-H, Qin X, Zhang D-W. Experimental study on the effect of compressor frequency on the performance of transcritical CO2 heat pump system with regenerator. Appl Therm Eng 2019;150:1216–23. https://doi.org/10.1016/j.applthermaleng.2019.01.091.
[102] Cao F, Wang Y, Ye Z. Theoretical analysis of internal heat exchanger in transcritical CO2 heat pump systems and its experimental verification. Int J Refrig 2019;106:506–16. https://doi.org/10.1016/j.ijrefrig.2019.05.022.
[103] Liao SM, Zhao TS, Jakobsen A. A correlation of optimal heat rejection pressures in transcritical carbon dioxide cycles. Appl Therm Eng 2000;20:831–41. https://doi.org/10.1016/S1359-4311(99)00070-8.
[104] Feng F, Zhang Z, Liu X, Liu C, Hou Y. The influence of internal heat exchanger on the performance of transcritical CO 2 water source heat pump water heater. Energies 2020;13:1–14. https://doi.org/10.3390/en13071787.
[105] Zhang XP, Fan XW, Wang FK, Shen HG. Theoretical and experimental studies on optimum heat rejection pressure for a CO2 heat pump system. Appl Therm Eng 2010;30:2537–44. https://doi.org/10.1016/j.applthermaleng.2010.07.003.
[106] Liu Y, Groll EA, Yazawa K, Kurtulus O. Energy-saving performance and economics of CO2 and NH3 heat pumps with simultaneous cooling and heating applications in food processing: case studies. Int J Refrig 2017;73:111–24. https://doi.org/10.1016/j.ijrefrig.2016.09.014.
[107] White SD, Yarrall MG, Cleland DJ, Hedley RA. Modelling the performance of a transcritical CO2 heat pump for high temperature heating. Int J Refrig 2002;25:479–86. https://doi.org/10.1016/S0140-7007(01)00021-4.
[108] Kimura T, Fuchikami H, Nishida K, Kudo M, Machida A, Saito K, et al. Development of a high temperature heat pump using reusable heat as the heat source. Kobe: JRAIA International Symposium; 2018. Paper 8.1.
[109] Verdnik M, Rieberer R. Experimental analysis of a R600 high-temperature heat pump in sub-critical and trans-critical operation. In: The 14th IIR Gustav Lorentzen Conference on Natural Manuel Verdnik refrigerants; 2020. Paper 1055.
[110] Liu Y, Groll EA, Yazawa K, Kurtulus O. Theoretical analysis of energy-saving performance and economics of CO2 and NH3 heat pumps with simultaneous cooling and heating applications in food processing. Int J Refrig 2016;65:129–41. https://doi.org/10.1016/j.ijrefrig.2016.01.020.
[111] Bellemo L, Gerritsen J, Hoffmann K. High temperature CO_2 heat pump integration into the spray drying process. 2nd Conference on High Temperature Heat Pumps - Book of Presentations; 2019. Paper 3.1.
[112] Hao Z, Yanting Z, Jingyu X, Lin W, Zheng H. Performance analysis of internal heat exchanger-based quasi-two-stage vapor compression heat pump system for high-temperature steam production. Energy Technol 2020;8:2000623. https://doi.org/10.1002/ente.202000623.
[113] Cavallini A, Cecchinato L, Corradi M, Fornasieri E, Zilio C. Two-stage transcritical carbon dioxide cycle optimisation: a theoretical and experimental analysis. Int J Refrig 2005;28:1274–83. https://doi.org/10.1016/j.ijrefrig.2005.09.004.
[114] Cecchinato L, Chiarello M, Corradi M, Fornasieri E, Minetto S, Stringari P, et al. Thermodynamic analysis of different two-stage transcritical carbon dioxide cycles. Int J Refrig 2009;32:1058–67. https://doi.org/10.1016/j.ijrefrig.2008.10.001.
[115] Sarkar J, Agrawal N. Performance optimization of transcritical CO2 cycle with parallel compression economization. Int J Therm Sci 2010;49:838–43. https://doi.org/10.1016/j.ijthermalsci.2009.12.001.
[116] Yang W, Cao X, He Y, Yan F. Theoretical study of a high-temperature heat pump system composed of a CO2 transcritical heat pump cycle and a R152a subcritical heat pump cycle. Appl Therm Eng 2017;120:228–38. https://doi.org/10.1016/j.applthermaleng.2017.03.098.
[117] Wu D, Hu B, Wang RZ. Performance simulation and exergy analysis of a hybrid source heat pump system with low GWP refrigerants. Renew Energy 2018;116:775–85. https://doi.org/10.1016/j.renene.2017.10.024.
[118] Zhu Y, Huang Y, Li C, Zhang F, Jiang P-X. Experimental investigation on the performance of transcritical CO2 ejector–expansion heat pump water heater

system. Energy Convers Manag 2018;167:147–55. https://doi.org/10.1016/j.enconman.2018.04.081.
[119] Elbel S, Hrnjak P. Experimental validation of a prototype ejector designed to reduce throttling losses encountered in transcritical R744 system operation. Int J Refrig 2008;31:411–22. https://doi.org/10.1016/j.ijrefrig.2007.07.013.
[120] Sun F, Ma Y. Thermodynamic analysis of transcritical CO2 refrigeration cycle with an ejector. Appl Therm Eng 2011;31:1184–9. https://doi.org/10.1016/j.applthermaleng.2010.12.018.
[121] Huang BJ, Jiang CB, Hu FL. Ejector performance characteristics and design analysis of jet refrigeration system. J Eng Gas Turbines Power 1985;107:792–802. https://doi.org/10.1115/1.3239802.
[122] Kornhauser AA. The use of an ejector as a refrigerant expander. International refrigeration and air conditioning conference, vol. 11; 1990. http://docs.lib.purdue.edu/cgi/viewcontent.cgi?article=1081&context=iracc.
[123] Sarkar J. Performance characteristics of natural refrigerants based ejector expansion refrigeration cycles. Proc IMechE; Pt A: Journal Power Energy 2009;223:543–50. https://doi.org/10.1243/09576509JPE753.
[124] Chen X, Zhou Y, Yu J. A theoretical study of an innovative ejector enhanced vapor compression heat pump cycle for water heating application. Energy Build 2011;43:3331–6. https://doi.org/10.1016/j.enbuild.2011.08.037.
[125] Boccardi G, Botticella F, Lillo G, Mastrullo R, Mauro AW, Trinchieri R. Experimental investigation on the performance of a transcritical CO2 heat pump with multi-ejector expansion system. Int J Refrig 2017;82:389–400. https://doi.org/10.1016/j.ijrefrig.2017.06.013.
[126] Nakagawa M, Marasigan AR, Matsukawa T. Experimental analysis on the effect of internal heat exchanger in transcritical CO2 refrigeration cycle with two-phase ejector. Int J Refrig 2011;34:1577–86. https://doi.org/10.1016/j.ijrefrig.2010.03.007.
[127] Zhang L, Xue B, Chen T, Li G. Silane functionalization on zeolite 13X surface for direct steam generation in a solid sorption heat pump. Energy Convers Manag 2021;244:114457. https://doi.org/10.1016/j.enconman.2021.114457.
[128] Xue B, Iwama Y, Tanaka Y, Nakashima K, Wijayanta AT, Nakaso K, et al. Cyclic steam generation from a novel zeolite–water adsorption heat pump using low-grade waste heat. Exp Therm Fluid Sci 2013;46:54–63. https://doi.org/10.1016/j.expthermflusci.2012.11.020.
[129] Nordtvedt SR. Hybrid heat pump for waste heat recovery in Norwegian food industry. International Heat Pump Conference 2011;6.
[130] Ahrens MU, Hafner A, Eikevik TM. Development of ammonia-water hybrid absorption- compression heat pumps. International Congress of Refrigeration 2019;8. https://doi.org/10.18462/iir.icr.2019.1869. https://doi.org/.
[131] Walmsley Timothy G, Klemes Jiri Jaromir, Walmsley Michael RW, Atkins Martin J, Varbanov Petar S. Innovative hybrid heat pump for dryer process integration. Chemical Engineering Transactions 2017;57:1039–44. https://doi.org/10.3303/CET1757174.
[132] Jensen JK, Markussen WB, Reinholdt L, Elmegaard B. Exergoeconomic optimization of an ammonia–water hybrid absorption–compression heat pump for heat supply in a spray-drying facility. Int J Energy Environ Eng 2015;6:195–211. https://doi.org/10.1007/s40095-015-0166-0.
[133] Sveine T, Grandum S, Bakaas H. Design of high temperature absorption/compression heat pump. Natural Working Fluids 1998:491–500.
[134] Klemeš JJ, Varbanov PS, Walmsley TG, Jia X. New directions in the implementation of Pinch methodology (PM). Renew Sustain Energy Rev 2018;98:439–68. https://doi.org/10.1016/j.rser.2018.09.030.
[135] Schlosser F, Wiebe H, Walmsley TG, Atkins MJ, Walmsley MRW, Hesselbach J. Heat pump Bridge analysis using the modified energy transfer diagram. 19961073 Energies 2021;14:137. https://doi.org/10.3390/en14010137. 137.
[136] Townsend DW, Linnhoff B. Heat and power networks in process design. Part I: criteria for placement of heat engines and heat pumps in process networks. AIChE J 1983;29:742–8. https://doi.org/10.1002/aic.690290508.
[137] Fu C, Gundersen T. Integrating compressors into heat exchanger networks above ambient temperature. AIChE J 2015;61:3770–85. https://doi.org/10.1002/aic.15045.
[138] Fu C, Gundersen T. A novel sensible heat pump scheme for industrial heat recovery. Ind Eng Chem Res 2016;55:967–77. https://doi.org/10.1021/acs.iecr.5b02417.